Dalton Transactions

ROYAL SOCIETY OF CHEMISTRY

PAPER

View Article Online
View Journal

Cite this: DOI: 10.1039/d1dt04091j

N,N'-Substituted thioureas and their metal complexes: syntheses, structures and electronic properties†

Ali A. A. Al-Riyahee,[a] Peter N. Horton,[b] Simon J. Coles,[b] Colin Berry,[c] Paul D. Horrocks,[d] Simon J. A. Pope *[a] and Angelo J. Amoroso*[a]

The synthesis of six *N,N'*-substituted thiourea ligands (L^{1a}–L^{3b}) was achieved in two steps. A corresponding extensive series of Cu(I), Cu(II), Ni(II) and Zn(II) complexes (**1–24**) with varying formulations were synthesised from these ligands by the reaction of a 1 : 1 or a 1 : 2 mixture of Cu(II), Ni(II) and Zn(II) perchlorate or chloride salts. Complexes **1–24** have been comprehensively characterised by mass spectrometry, elemental analysis, UV-vis., IR, and ^{1}H and ^{13}C{^{1}H} NMR spectroscopies where applicable. The X-ray crystal structures were obtained for eight examples: $[(L^{1a})_2Cu]ClO_4$ (**1**), $[(L^{1c})_2Zn](ClO_4)_2$ (**4**), $[(L^{2a})_2Cu]ClO_4$ (**6**), $[(L^{2c})_2Ni](ClO_4)_2$ (**7**), $[(L^{1b})_2Cu](ClO_4)$ (**15**), $[(L^{1b})CuCl]$ (**16**), $[(L^{4})_2CuCl_2]$ (**19**) and $[(L^{3b})CuClO_4]$ (**21**). These studies reveal that L^{1c} and L^{2c} represent ligands that have undergone cleavage during reaction with the metal salt; L^{4} represents an intramolecular rearrangement (*via* a Hugershoff reaction) of L^{2b}; and in most cases Cu(II) is reduced to Cu(I) during the ligand reaction. The X-ray crystal structures also reveal that **1**, **4**, **6**, **15** and **16** are monometallic species in the solid state; that Cu(I) in **1**, **6, 15** and **16** and Zn(II) in **4** are arranged in a distorted tetrahedral geometry; that Cu(I) in **21** adopts a trigonal planar geometry; and that in **7** and **19** the Ni(II) and Cu(II) centres, respectively, possess square planar geometry. Preliminary studies on the biological activity (using the Malaria Sybr Green I Fluorescence assay) of the thiourea containing complexes suggests that the d^{10} complexes, and increased ligand stoichiometries, may afford higher potency.

Received 3rd December 2021,
Accepted 30th January 2022

DOI: 10.1039/d1dt04091j

rsc.li/dalton

Introduction

The acylthiourea group is a versatile and readily synthesised functional group which has been utilised in synthesis and incorporated into various molecules, including co-ordination complexes. Such systems have attracted significant attention due to these complexes having potential applications in medicinal chemistry as pesticides,[1] bacteriocides,[2,3] antiviral,[4] antihelmintic,[5] antifungal[6] and antimalarial[7] compounds. Additionally, specific studies have shown a variety of acyl thiourea compounds to be extremely important in a biological context as they are, for example: (i) selective inhibitors of platelet-derived growth factor (PDGF) receptor;[8] (ii) potent inhibitors of the Hedgehog signaling pathway;[9] (iii) a c-Met (RTK or HGFR) inhibitor, for deactivating mechanisms by which various tumours and cancer stem cells promote angiogenesis and metastasis;[10] and (iv) an HDAC8 activator in non-catalytic HDAC8 mutants for research models of cohesinopathies.[11]

In addition to these biological applications, the structural rigidity of the acylthiourea group and its potential as a multiple hydrogen bond donor has prompted investigations into its behaviour as an anion binder,[12] including *via* a multi-array of hydrogen bond donors,[13] and as a ligand for the construction of polynuclear complexes.[14]

In its role in co-ordination chemistry the acylthiourea group is potentially a bidentate ligand, co-ordinating to metal ions *via* both the hard oxygen and soft sulfur donor atoms.[15,16] Alternatively, the ligand may form a strong intramolecular hydrogen bond between the carbonyl oxygen and a NH group in the thiourea, which induces a monodentate ligand bonding mode *via* the sulfur atom only, thus favouring soft metal ions.[2,3,17,18] When an additional donor atom (*e.g.* pyridine) is

[a]*School of Chemistry, Main Building, Cardiff University, Cardiff CF10 3AT, UK. E-mail: popesj@cardiff.ac.uk, amorosoaj@cardiff.ac.uk*
[b]*UK National Crystallographic Service, Chemistry, Faculty of Natural and Environmental Sciences, University of Southampton, Highfield, Southampton, SO17 1BJ, UK*
[c]*School of Biosciences, Cardiff University, CF10 3AT, UK*
[d]*Institute for Science and Technology in Medicine, Keele University, Staffordshire ST5 5BG, UK*

†Electronic supplementary information (ESI) available. CCDC 2082368 (**1**), 2082369 (**4**), 2082370 (**6**), 2082371 (**7**), 2082372 (**15**), 2082373 (**16**), 2082374 (**19**), 2082375 (**21**). For ESI and crystallographic data in CIF or other electronic format see DOI: 10.1039/d1dt04091j

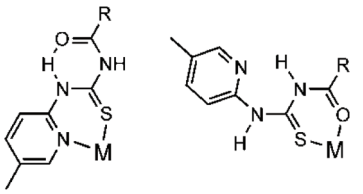

Fig. 1 Common bidentate co-ordination modes of pyridyl-acylthioureas.

placed on the thiourea framework, the ligand can then bind in a bidentate fashion in both cases, as shown in Fig. 1, with the structures observed being dependent on the nature of the metal ion.

With widespread and important biological activity, it is clearly advantageous to be able to modify these acylthiourea derived ligands and understand their co-ordination chemistry to a variety of metal centres. Clearly a better understanding of the nature of these complexes and properties is of potential value. Herein, we present an extensive structural and spectroscopic investigation into a series of metal complexes that incorporate the acylthiourea moiety. Importantly, we report interesting reactivities that can result in ligand cleavage and rearrangements which will have significant implications in the design and biological application of such systems in the future.

Results and discussion

Ligand synthesis

Two series of substituted thiourea derived ligands were prepared. The synthesis of $\mathbf{L^{1a}}$–$\mathbf{L^{3a}}$ and $\mathbf{L^{1b}}$–$\mathbf{L^{3b}}$ required the preparation of the benzoyl isothiocyanate and pivaloyl isothiocyanate precursors through the reaction of the corresponding acid chloride with potassium thiocyanate. The target ligands $\mathbf{L^{1a}}$–$\mathbf{L^{3a}}$ and $\mathbf{L^{1b}}$–$\mathbf{L^{3b}}$ were obtained by reaction of either 2-amino-5-methyl pyridine or 2,6-diaminopyridine with benzoyl isothiocyanate or pivaloyl isothiocyanate in acetonitrile (Scheme 1). The purification and recrystallisation approaches for these various ligands are described in the Experimental section. All samples were gently heated under vacuum prior to elemental analyses.

Co-ordination chemistry

The chelating properties of the new ligands were investigated using a variety of Cu(II), Ni(II), and Zn(II) sources. Schemes 2–7 provide the reaction conditions for the proposed complex formulations. Table 1 also summarises the isolated complexes and their respective ligand formulations obtained in this study.

For example, reaction of the different ligands with Cu $(ClO_4)_2{\cdot}6H_2O$ in a 2 : 1 stoichiometry was carried out in DMF/water at room temperature, yielding Cu(I) complexes of $\mathbf{L^{1a}}$ and $\mathbf{L^{1b}}$ (**1** and **15**), $\mathbf{L^{2a}}$ and $\mathbf{L^{2b}}$ (**6** and **18**), $\mathbf{L^{3a}}$ and $\mathbf{L^{3b}}$ (**12** and **22**). In all cases, analytical, spectral and crystallographic data (dis-

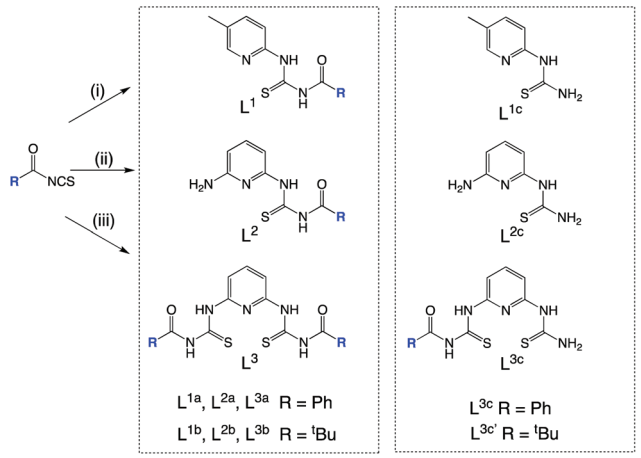

Scheme 1 Left: synthesis of the ligands: (i) 1 equiv. 2-amino-5-methyl-pyridine, MeCN, reflux; (ii) 1 equiv. 2,6-diaminopyridine, MeCN, reflux; (iii) 0.5 equiv. 2,6-diaminopyridine, MeCN, reflux. Inset right: the structures of fragmented ligand variants obtained during the co-ordination chemistry.

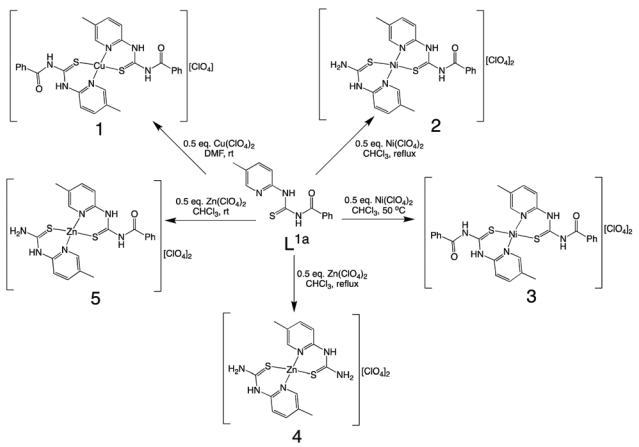

Scheme 2 Synthesis of complexes **1**–**5** from $\mathbf{L^{1a}}$.

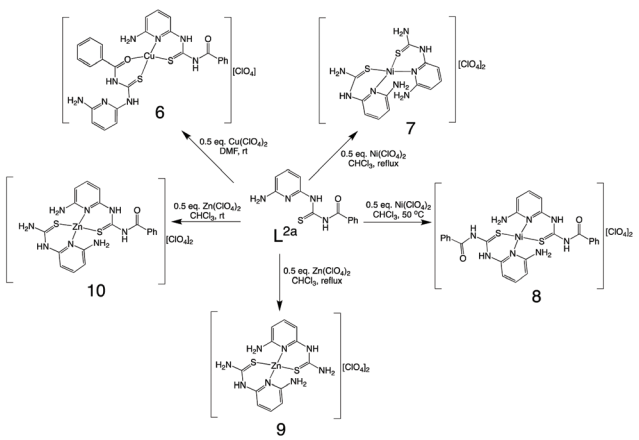

Scheme 3 Synthesis of complexes **6**–**10** from $\mathbf{L^{2a}}$.

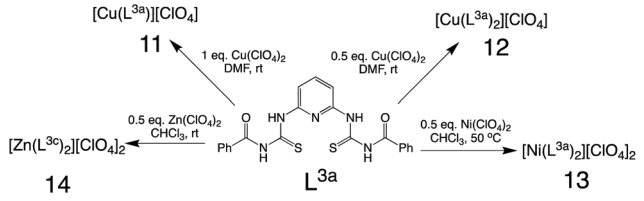

Scheme 4 Synthesis of complexes **11–14** from L^{3a}.

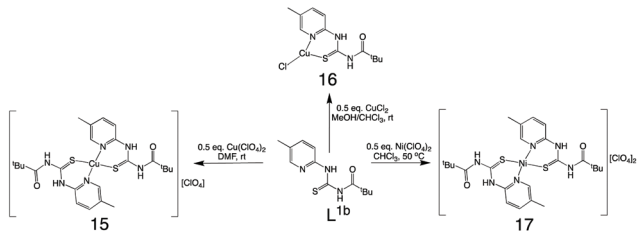

Scheme 5 Synthesis of complexes **15–17** from L^{1b}.

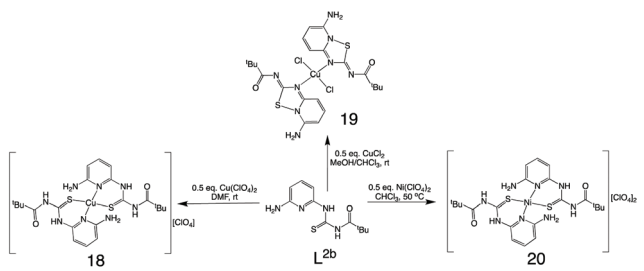

Scheme 6 Synthesis of complexes **18–20** from L^{2b}.

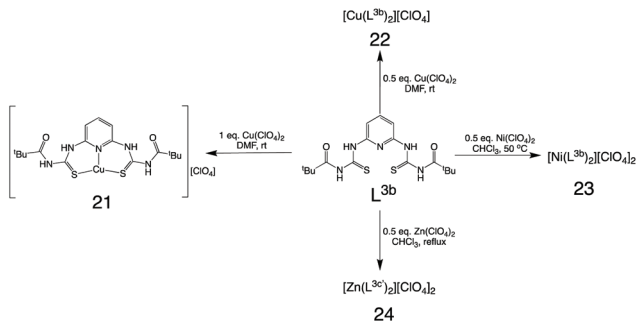

Scheme 7 Synthesis of complexes **21–24** from L^{3b}.

cussed later) indicated the reduction of the source Cu(II) to form $[Cu(L)_2](ClO_4)$ species. These Cu(I) complexes were isolated as red, orange or yellow solids, and were stable at room temperature. In the cases of L^{3a} and L^{3b}, when the reaction was repeated using a metal : ligand ratio of 1 : 1, Cu(I) complexes **11** and **21** were successfully isolated in the form of $[Cu(L)](ClO_4)$.

Interestingly, using $CuCl_2$ instead of $Cu(ClO_4)_2{\cdot}6H_2O$ with L^{2b} resulted in a Cu(II) complex, **19**, where the ligand had undergone a transformation to give L^4 (Scheme 6). The characterization of **19** revealed that the pyridylthiourea group of the ligand had undergone a Hugershoff reaction.[19,20] Previously, the oxidation of pyridylthioureas by bromine has been reported to yield the related heterocyclic 1,2,4-thiadiazolo[2,3-*a*]pyridine[21,23] and here it is assumed that $CuCl_2$ acts as an oxidant that promotes the rearrangement of the ligand. We postulate that formation of L^4, which results in the loss of the thiourea donor, is subsequently less suitable for supporting a Cu(I) centre. The analysis of **19**, supported by X-ray crystallographic studies (see below), suggests the Cu(II) ion is four co-ordinate with two trans arranged monodentate L^4 ligands and two co-ordinated chloride ions. While not in the scope of this current work, clearly future studies will address the limitations of this reaction with related ligands and varying conditions.

Reaction of the ligands with $Ni(ClO_4)_2{\cdot}6H_2O$ in a 2 : 1 ratio were initially undertaken at 75 °C in $CHCl_3$/methanol. Characterisation of these Ni(II) complexes indicated cleavage (these coordinated ligands are thus referred to as L^{1c}, L^{2c}, L^{3c}) of one or two of the benzoyl or pivaloyl groups (see Scheme 1). Repeating the reaction at 50 °C prevented cleavage of these groups and gave the anticipated complexes. The Ni(II) complexes were collected as brown or green coloured solids and were stable at room temperature.

Mononuclear Zn(II) complexes were formed as colourless powders by the reaction of the ligands with $Zn(ClO_4)_2{\cdot}6H_2O$ (2 : 1 molar ratio) in a mixture of $CHCl_3$/methanol at room temperature and 75 °C. As observed with the Ni(II) co-ordination chemistry, the Zn(II) complexes again formed with cleavage (giving complexes of L^{1c}, L^{2c}, L^{3c}) of one or both acyl moieties from the co-ordinated ligands. In contrast to the analogous Ni(II) chemistry, repeating the reactions at lower temperatures did not prevent cleavage of these groups.

Table 1 Summary of the metal complexes isolated in this work

Complex	Metal	Ligand(s)	Complex	Metal	Ligand(s)
1	Cu(I)	L^{1a}	**13**	Ni(II)	L^{3a}
2	Ni(II)	L^{1a}, L^{1c}	**14**	Zn(II)	L^{3c}
3	Ni(II)	L^{1a}	**15**	Cu(I)	L^{1b}
4	Zn(II)	L^{1c}	**16**	Cu(I)	L^{1b}, Cl
5	Zn(II)	L^{1a}, L^{1c}	**17**	Ni(II)	L^{1b}
6	Cu(I)	L^{2a}	**18**	Cu(I)	L^{2b}
7	Ni(II)	L^{2c}	**19**	Cu(II)	L^4
8	Ni(II)	L^{2a}	**20**	Ni(II)	L^{2b}
9	Zn(II)	L^{2c}	**21**	Cu(I)	L^{3b} (1 : 1)
10	Zn(II)	L^{2a}, L^{2c}	**22**	Cu(I)	L^{3b} (2 : 1)
11	Cu(I)	L^{3a} (1 : 1)	**23**	Ni(II)	L^{3b}
12	Cu(I)	L^{3a} (2 : 1)	**24**	Zn(II)	$L^{3c'}$

X-ray crystallography studies

X-ray crystal structures of $[Cu(L^{1a})_2]ClO_4{\cdot}CH_3CN$ (1) and $[Cu(L^{1b})_2]ClO_4{\cdot}H_2O$ (15). Red, monoclinic crystals of **1** and orange orthorhombic crystals of **15** were obtained by vapour diffusion of diethyl ether into an acetonitrile solution of **1**, or a chloroform solution of **15**. Selected bond distances and bond angles are given in Table 2. Fig. 2 shows **1**, with the metal centre tetrahedrally coordinated by two bidentate ligands.

Table 2 Selected bond lengths and angles for structures **1** and **15**

Compound **1**			
Bond length (Å)			
Cu1–N1	2.074(2)	Cu1–S21	2.2191(7)
Cu1–N21	2.079(2)	Cu1–S1	2.2235(7)
Bond angles (°)			
N1–Cu1–N21	111.87(9)	N21–Cu1–S21	98.12(6)
N1–Cu1–S21	111.55(6)	N1–Cu1–S1	98.04(6)
N21–Cu1–S1	109.21(6)	S21–Cu1–S1	128.23(3)
Compound **15**			
Bond length (Å)			
Cu1–N1	2.054(7)	Cu1–S21	2.213(2)
Cu1–N21	2.050(6)	Cu1–S1	2.231(2)
Bond angles (°)			
N1–Cu1–N21	110.9(3)	N1–Cu1–S1	97.41(18)
N1–Cu1–S21	116.06(18)	N21–Cu1–S1	109.83(18)
N21–Cu1–S21	98.88(18)	S21–Cu1–S1	123.97(9)

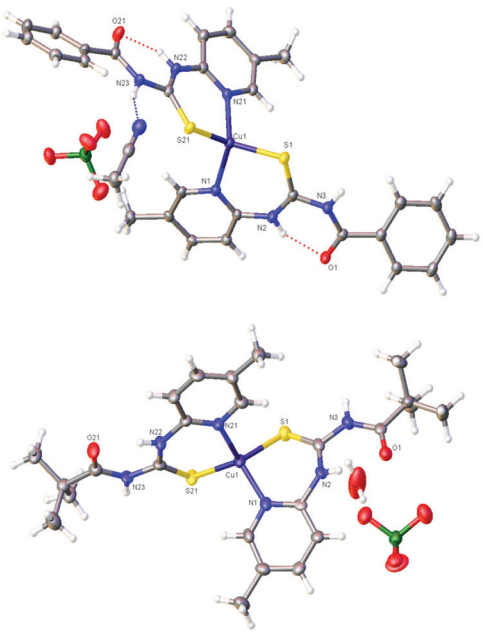

Fig. 2 The asymmetric units of **1** (top) and **15** (bottom). Displacement ellipsoids are shown at 50% probability.

Each ligand co-ordinates *via* a pyridine ring and the sulfur of the thiourea. Bond angles about the Cu(I) centre range from 98.04(6)–128.23(3) degrees, demonstrating a significant distortion from an ideal tetrahedral geometry. The most acute of these angles (N1–Cu1–S1 and N21–Cu1–S21) are associated with the bond angles between the two donors of each bidentate ligand. The largest bond angle is observed for S21–Cu1–S1 (128.23(3)°). These observations are in line with previous work: of the four previously reported Cu(I) crystal structures of pyridyl thiourea derivatives,[22] all were tetrahedral and the metal ion was coordinated by the pyridyl group and the sulfur donor. Typical for this class of ligand, intermolecular hydrogen bond interactions were also observed. More specifically, and typical of acyl thioureas, hydrogen bonding between the C=O and an N–H group results in the formation of a six-membered ring (N2–H2···O1 and N22–H22···O21). Furthermore, there are additional weaker intermolecular hydrogen bonds between the ligand and the perchlorate counter anion.

X-ray crystal structure of $[Zn(L^{1c})_2](ClO_4)_2$ (4). Monoclinic colourless crystals of **4** were obtained by vapour diffusion of diethyl ether into an acetonitrile solution of **4** (Fig. 3). Selected bond distances and bond angles are given in Table 3. The complex crystallises in the monoclinic space group $P2_1$. The Zn (II) ion displays a tetrahedral geometry, with bond angles about the metal centre ranging from 99.33(14)–115.51(18)°. The variation from tetrahedral geometry is less pronounced that that seen in **1** and **15**. The metal ion in **4** is co-ordinated by two bidentate ligands *via* pyridine and sulfur donor atoms. The structure clearly shows that the ligand has hydrolysed in the reaction to give L^{1c} and benzoic acid. There are extensive intermolecular hydrogen bond interactions between the complex and the perchlorate counter-ions. One interaction is between a thiourea, acting as a bidentate hydrogen bond donor, and a perchlorate (N1–H1b···O22, N2–H2···O23) and the other interaction is a perchlorate ion hydrogen bonding with two separate thioureas, each acting as a monodentate donor (N1–H1a···O31^{i} and N11–H11b^{i}···O32) were observed between the thiourea N–H and the perchlorate oxygen atom. (Symmetry transformation to generate O31^{i}: $x + 1, y, z$.)

X-ray crystal structure of $[Cu(L^{2a})_2]ClO_4$ (6). Monoclinic dark orange crystals of **6** were obtained by vapour diffusion of diethyl ether into an acetonitrile/methanol (2 : 1) solution of the complex. The molecular structure of the complex $[Cu(L^{2a})_2]ClO_4$ (**6**) was established by X-ray crystallography and is illustrated in Fig. 4, along with key bond lengths and angles in Table 4. The Cu(I) centre is chelated by two L^{2a} ligands resulting in a distorted structure with three short Cu–S or Cu–N bonds and one longer Cu–O bond (2.3703(16) Å). Of note, L^{2a} and L^{1a} are similar except for the substitution of the pyridine ring, with L^{1a} having a methyl group in the 5-position and L^{2a} an amino group in the 6-position. These groups play no direct role in the co-ordination of the metal centre, and the amino

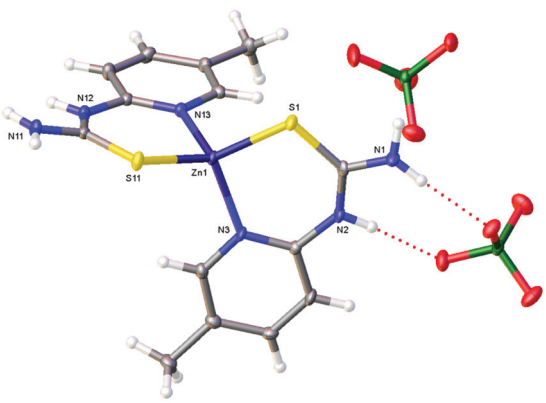

Fig. 3 The asymmetric unit of **4**. Displacement ellipsoids are shown at 50% probability.

Table 3 Selected bond lengths and angles for structure **4**

Bond length (Å)			
Zn1–N3	2.021(5)	Zn1–S11	2.2535(15)
Zn1–N13	2.025(5)	Zn1–S1	2.2596(16)
Bond angles (°)			
N3–Zn1–N13	115.51(18)	N3–Zn1–S1	99.73(14)
N3–Zn1–S11	114.13(14)	N13–Zn1–S1	113.64(14)
N13–Zn1–S11	99.33(14)	S11–Zn1–S1	115.37(5)

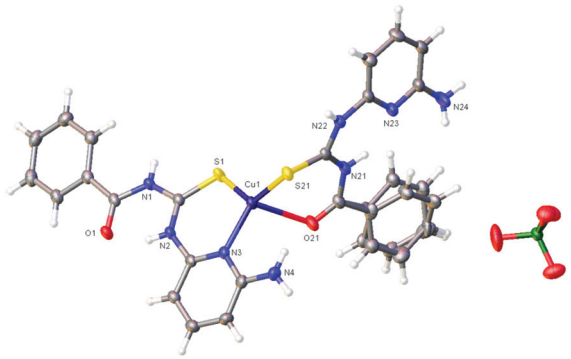

Fig. 4 The asymmetric unit of **6**. Displacement ellipsoids are shown at 50% probability.

Table 4 Selected bond lengths and angles for structure **6**

Bond length (Å)			
Cu1–N3	2.0148(17)	Cu1–S21	2.2515(6)
Cu1–S1	2.2127(6)	Cu1–O21	2.3703(16)
Bond angles (°)			
N3–Cu1–S1	102.76(5)	N3–Cu1–O21	101.80(6)
N3–Cu1–S21	125.50(5)	S1–Cu1–O21	109.06(5)
S1–Cu1–S21	126.94(2)	S21–Cu1–O21	83.50(4)

group does not appear to be involved in any strong hydrogen bonding interactions, suggesting the differences between the two structures, **1** and **6**, appears to be due to the differing steric demands of the two ligands. More specifically, the greater steric demand of $\mathbf{L}^{2a}$ results in the ligand having two different co-ordination modes in **6**. One ligand co-ordinates to the metal in an identical manner to that observed in **1**, while the second ligand also co-ordinates in a bidentate manner, but through the sulfur and oxygen donors. In this co-ordination mode, the pyridine nitrogen is now forming an intramolecular hydrogen bond with the thiourea NH groups (N21–H21···N23). Presumably, the soft Cu(I) centre forms the Cu(I)–O interaction in the absence of other possible softer donors. The Cu–O bond is significantly longer than the other Cu-donor interactions and this 3 + 1 interaction might be considered as a trigonal planar structure or as a highly distorted tetrahedral geometry.

X-ray structures of $[Ni(L^{2c})_2](ClO_4)_2{\cdot}H_2O{\cdot}EtOH$ (7). Monoclinic red coloured crystals of **7** were obtained by vapour diffusion of diethyl ether into an ethyl acetate solution of **7**. The

Table 5 Selected bond lengths and angles for structure **7**

Bond length (Å)			
Ni1–N3	1.923(2)	Ni1–S1	2.1647(8)
Ni1–N3′	1.922(2)	Ni1–S1′	2.1647(8)
Bond angles (°)			
N3–Ni1–N3′	92.25(14)	S1–Ni1–S1′	87.80(4)
N3′–Ni1–S1	169.76(7)	N3′–Ni1–S1′	90.84(7)
N3–Ni1–S1	90.85(7)	N3–Ni1–S1′	169.76(7)

Symmetry transformations used to generate equivalent atoms: #1 $-x + 1, y, -z + 1/2$.

selected bond distances and bond angles are given in Table 5 and the structure of **7** is shown in Fig. 5. The complex contains two bidentate ligands, each demonstrating loss of the benzoyl group. The ligands again co-ordinate through the pyridine ring and sulfur atom of the thiourea. The Ni(II) complex has a slightly distorted square planar geometry: the torsion angle between the four donors range from 13.4–14.5(5)° with bond angles about the metal centre ranging from 88.08(3)–92.55(9)° and *trans* angles of 169.95(6)° and 170.57(6)°. The observed Ni(II)–S/Ni(II)–N bond lengths are in the expected range.[2]

X-ray structure of $[Cu(L^{1b})Cl]$ (16). Monoclinic red crystals of **16** were obtained by vapour diffusion of diethyl ether into a $CHCl_3$ solution of the complex. Selected bond lengths and angles are listed in Table 6 and the structure is shown in Fig. 6. Each copper atom is co-ordinated by two bidentate ligands where one ligand binds through a sulfur atom and a

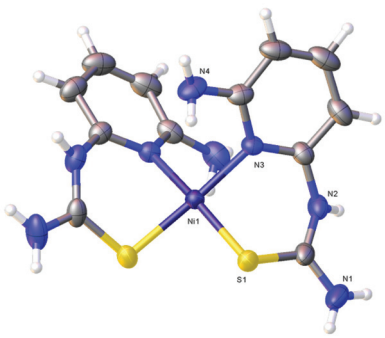

Fig. 5 The asymmetric unit of **7**. Displacement ellipsoids are shown at 50% probability.

Table 6 Selected bond lengths and angles for structure **16**

Bond length (Å)			
Cl1–Cu1	2.2504(5)	Cu1–S1^{i}	2.2881(6)
Cu1–N1	2.0863(17)	Cu1–S1	2.3080(5)
Bond angles (°)			
N1–Cu1–Cl1	112.57(5)	N1–Cu1–S1	92.15(5)
N1–Cu1–S1^{i}	103.38(5)	Cl1–Cu1–S1	114.25(2)
Cl1–Cu1–S1^{i}	114.59(2)	S1^{i}–Cu1–S1	116.958(13)

Symmetry transformations used to generate equivalent atoms: #1 $-x + 1, y - 1/2, -z + 1/2$.

pyridine donor. The sulfur donor also co-ordinates to a second Cu(I) centre, and this arrangement is reciprocated by another complex unit leading to the formation of a polymeric chain. The Cu(I) co-ordination sphere is completed by a chloride atom. Bond angles about the metal centre range from 92.15(5)–116.958(13)°, and as expected, the most acute angle is that formed by the two donors within the same ligand (N1–Cu1–S1: 92.13(5)°), but it is slightly more acute than the analogous bite angles observed in **1** and **15**. An intramolecular hydrogen bond is again observed in the acyl thiourea moiety (1.83 Å) and this is similar to that observed for **1** and **15**. The structure observed for **16** is similar to the polymeric tetrahedral complex $[Cu(L)Br]_n$ (L = *N*-(2-pyridyl)-*N*′-phenylthiourea) reported by Saxena.[23]

X-ray structure of $[Cu(L^4)_2Cl_2]$ (19). Monoclinic dark orange crystals of 19 were obtained by vapour diffusion of diethyl ether into a dichloromethane : ethanol (1 : 1) solution of 19. Selected bond distances and bond angles are given in Table 7 and the structure is shown in Fig. 7. The Cu(II) complex is clearly square planar with bond angles about the metal centre 89.28(6)–90.72(6) and two bond angles at 180.00 degrees, with the Cu centre lying in a special position, at the centre of symmetry about the complex. A related complex $[(X)_2CuCl_2]$ (X = (*N*-(7-methyl-2*H*-[1,2,4]thiadiazolo[2,3-*a*]pyridine-2-ylidene) benzamide) reported by Adhami *et al.* exhibited the same N_2Cl_2 square planar coordination environment, with similar bond lengths (Cu–Cl1 2.2637(14), Cu–N2 1.988(2) Å).[24] Intramolecular hydrogen bonding (N4–H4A···S1, 2.62 Å) was also observed within the heterocycle with two weak intermolecular interactions (N4–H4A···Cl1ii and N4–H4B···Cl1iii 2.53(4) and 2.54(4) Å). (Symmetry transformations used to generate equivalent atoms: Cl1ii: x, $-y + 1/2$, $z + 1/2$; Cl1iii: $-x + 2$, $y - 1/2$, $-z + 1/2$.

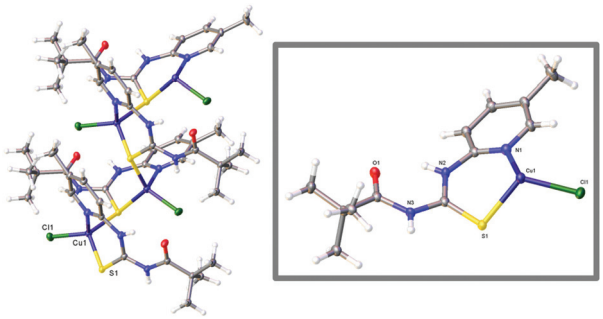

Fig. 6 The polymeric nature of **16**, with the co-ordination sphere of Cu (I) shown inset.

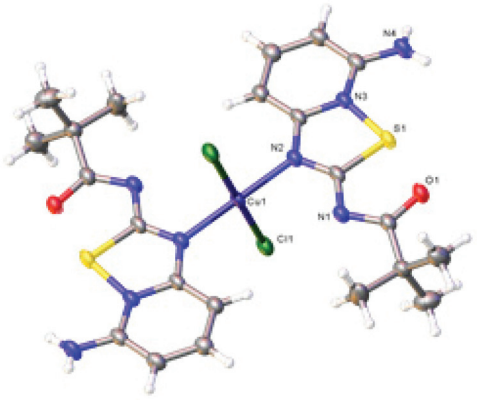

Fig. 7 The asymmetric unit of **19**. Displacement ellipsoids are shown at 50% probability.

X-ray structure of $[Cu(L^{3b})](ClO_4)$ (21). Monoclinic yellow crystals of **21** were obtained by vapour diffusion of diethyl ether into an ethanol : dichloromethane (3 : 1) solution of **21**. Selected bond lengths and angles are given in Table 8. The metal centre (Fig. 8) is co-ordinated by a single ligand that acts as a tridentate ligand through a nitrogen pyridine ring and the sulfur atoms of the two thioureas. The Cu(I) centre is approximately trigonal planar, although the bond angles around Cu(I) (107.40(18), 107.69(18) and 144.87(7)°) highlight the distortion caused by the strain in the six-membered chelate rings. This geometry is not uncommon for Cu(I), and an analysis of monodentate homoleptic donor sets with Cu(I) has revealed a significant propensity to form trigonal planar complexes,[25] and examples exist for Cu(I) trigonal planar complexes with a NS_2 donor set.[26,27]

Spectroscopic characterization of the complexes

^{1}H and ^{13}C{^{1}H} NMR spectroscopy. The ^{1}H and ^{13}C{^{1}H} NMR chemical shifts for the free ligands and their respective Cu(I), Ni(II) and Zn(II) complexes are listed in the Experimental section. For comparison, the chemical shifts for the two signature N*H* resonance (CON*H* and CSN*H*, the latter being hydrogen bonded) were observed around 11.53–11.85 and 12.99–13.22 ppm in L^{1a}–L^{3a} and around 10.58–10.90 and

Table 7 Selected bond lengths and angles for structure **19**

Bond length (Å)			
Cu1–Cl1	2.3047(6)	Cu1–Cl1^i	2.3047(6)
Cu1–N2^i	1.962(2)	Cu1–N2	1.962(2)
Bond angles (°)			
N2^i–Cu1–N2	180.00(3)	N2^i–Cu1–Cl1	90.75(6)
N2^i–Cu1–Cl1^i	89.25(6)	N2–Cu1–Cl1	89.25(6)
N2–Cu1–Cl1^i	90.75(6)	Cl1^i–Cu1–Cl1	180.0

Symmetry transformations used to generate equivalent atoms: #1 $-x + 2$, $-y + 1$, $-z + 1$.

Table 8 Selected bond lengths and angles for structure **21**

Bond length (Å)			
Cu1–N1	1.992(5)	Cu1–S2	2.141(2)
Cu1–S1	2.140(2)		
Bond angles (°)			
N1–Cu1–S1	107.54(18)	C1–N1–Cu1	121.4(5)
N1–Cu1–S2	107.56(18)	C6–S1–Cu1	102.1(2)
S1–Cu1–S2	144.87(7)	C8–S2–Cu1	101.3(3)
C5–N1–Cu1	120.9(5)		

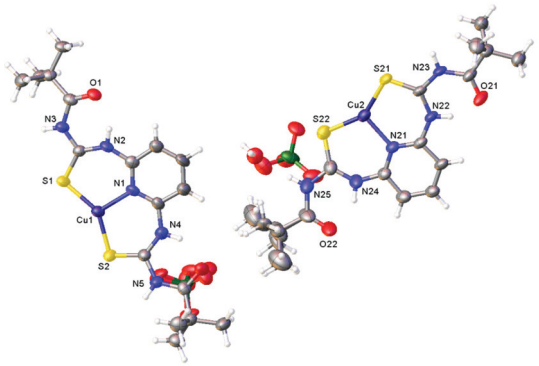

Fig. 8 The asymmetric unit of **21**. Displacement ellipsoids are shown at 50% probability.

12.93–13.19 ppm in $\mathbf{L^{1b}}$–$\mathbf{L^{3b}}$. Upon co-ordination, the CSN*H* and CON*H* resonances in the Cu(I), Ni(II) and Zn(II) complexes were shifted to 14.10–11.99 and 11.74–8.94 ppm, respectively for Cu(I) complexes, 13.24–10.61 and 11.71–10.46 for Ni(II) complexes and 12.93–10.46 and 10.61–8.82 ppm for Zn(II) complexes. ^{1}H NMR spectra for complexes **2**, **4**, **5**, **7**, **9**, **10** and **14** showed new peaks in the range 10.00–10.47 and 8.66–9.00 ppm, which were assigned to the –NH_2 groups that were formed from the cleavage of the benzoyl/pivaloyl groups. Consistent with this observation, the ^{1}H NMR spectra for these complexes also show the disappearance of the proton signals of the phenyl or *tert*-butyl groups in complexes **2**, **4**, **5**, **7**, **9**, **10** and **14**.

The ^{13}C{^{1}H} NMR spectra of the ligands and complexes showed the expected number of resonances at typical chemical shifts. For $\mathbf{L^{1a}}$–$\mathbf{L^{3a}}$, signature resonances due to C=O and C=S appeared at 168.48–168.92 and 177.09–178.47 ppm, respectively; for $\mathbf{L^{1b}}$–$\mathbf{L^{3b}}$ they appear further downfield at 176.86–178.30 and 180.34–180.65 ppm, respectively. In the complexes, these resonances shift significantly indicating co-ordination of the ligands to the metal centre *via* the S donor of the thiourea group. ^{13}C{^{1}H} NMR spectra for complexes **4**, **7**, and **9** showed the loss of the C=O signals consistent with the cleavage of the benzoyl/pivaloyl groups from those ligands.

Infrared spectra. IR spectra were recorded in the solid state. The spectra of the free ligands ($\mathbf{L^{1a}}$–$\mathbf{L^{3b}}$) showed characteristic bands at 3298–3485 (for N–H), 1672–1692 (C=O), 1468–1512 (C=N) and 1325–1366 cm^{-1} (C=S). The IR spectra of thiourea complexes (**1–24**) showed these absorption bands at 3267–3485 (N–H), 1636–1692 (C=O), 1439–1504 (C=N) and 1252–1287 cm^{-1} (C=S). In particular, a weakening of the C=S bond upon co-ordination is consistent with these observations. The IR spectra of complexes of $\mathbf{L^{2a}}$ (**6** and **8**) show considerable lowering of the C=O stretching frequency (~1660 cm^{-1} *cf* ~1670 cm^{-1}), suggesting co-ordination with the metal centre through the carbonyl group, which is consistent with solid state the X-ray structure for **6**. Complex **20** has a C=O stretching frequency of 1664 cm^{-1} suggesting that this ligand binds in a similar manner (bidentate through O and S). For complexes **4**, **7**, and **9**, the most striking change is the loss of the C=O indicating cleavage of the benzoyl and pivaloyl groups from the complexes. The complexes **1–3**, **5**, **10–17**, **18** and **21–23** show little change in C=O stretching frequency when compared to the corresponding free ligand, implying the carbonyl group is non-co-ordinating for these complexes. The presence of two characteristic bands at 1053–1096 and 621–627 cm^{-1} indicated that the T_d symmetry of ClO_4^- is maintained in all cationic complexes and thus implies non-co-ordinating ClO_4^-.[28,29]

Electronic spectra. The UV-vis. spectra of the ligands $\mathbf{L^{1a}}$–$\mathbf{L^{3b}}$ and their complexes were recorded as DMF solutions and their full data are presented in the Experimental section. Spectra of the free ligands $\mathbf{L^{1a}}$–$\mathbf{L^{3b}}$ showed strong absorption bands at λ_{max} 214–293 nm and 299–367 nm which are attributed to the presence of allowed ligand-centred $\pi \rightarrow \pi^*$ transitions. The corresponding spectra for the d^{10} Cu(I) and Zn(II) complexes are thus dominated by the ligand-centred bands in the UV region, with minor shifts noted upon coordination. In contrast, the spectra for the square planar Ni(II) complexes **2**, **3**, **7**, **8**, **17** and **20** also display weaker additional bands between 390–421 nm (*ca.* 400 M^{-1} cm^{-1}) and around 584–612 nm (<100 M^{-1} cm^{-1}). The latter of these bands is likely to be the d(xy) → d($x^2 - y^2$) transitions which is in good agreement with previously reported Ni(II) complexes.[30,31] The spectra of the six co-ordinate, pseudo octahedral Ni(II) complexes **13** and **23** also showed two very weak d–d bands in the visible and near-IR region, assigned to the $^3A_{2g} \rightarrow {}^3T_{1g}(F)$ and $^3A_{2g} \rightarrow {}^3T_{2g}$ transitions, respectively. From these ligand field spectra it was possible to deduce (assuming O_h geometry) Dq, B and β parameters, of 1068 cm^{-1}, 855 cm^{-1} and 0.82 for **13**, and 1050 cm^{-1}, 875 cm^{-1} and 0.84 for **23** (Fig. 9).

Magnetic susceptibility measurements. The observed magnetic moments of Ni(II) complexes **2**, **3**, **7**, **8**, **17** and **20** were measured using the Evan's method and suggest a diamagnetic square planar structure, while the magnetic moments for complexes **13** and **23** are 2.94 and 2.98 BM and, though lower than might be expected, are more consistent with a pseudo octahedral geometry at Ni(II). The magnetic moment of complex **19** is 1.80 BM, consistent with a Cu(II) oxidation state.

Electrochemical measurements. The electrochemical data for Cu(I), Cu(II) and Ni(II) complexes were measured in acetonitrile using [Bu_4N][PF_6] (0.1 M) as supporting electrolyte. The

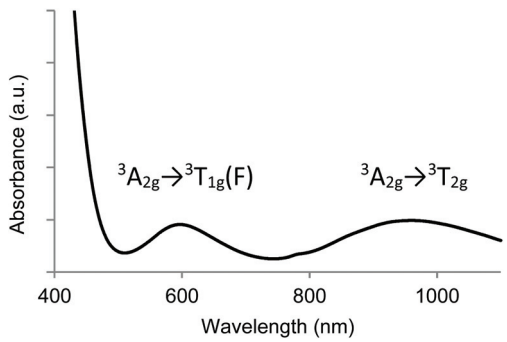

Fig. 9 Electronic spectrum of the nickel complex **23** (DMF, room temperature).

cyclic voltammograms of the Cu(I) complexes **1**, **6**, **11**, **12**, **15**, **16**, **18**, **21** and **22** are very similar, typically showing a quasi-reversible process between −0.20 to −0.45 V (*vs.* Fc/Fc^+) with large peak-to-peak separations being observed (200–350 mV). This potential is typical for a Cu(I)/Cu(II) couple and the peak to peak separations, being much greater than those observed with the ferrocene internal standard, suggest a quasi-reversible nature. This is possibly due to a structural/geometric rearrangement induced between the Cu(I) and Cu(II) oxidation states and their resultant geometric preferences. Furthermore, it was noted that the application of high negative potentials for prolonged periods caused a sharp anodic peak between −0.5 to −0.7 V suggestive of a species being deposited upon the electrode. All Cu(I) complexes except **16** showed an irreversible oxidative process in the range +0.520 to +1.08 V. Interestingly, **19** was unique among these copper complexes as the voltammogram displayed a single reversible process at +0.250 V *vs.* Fc/Fc^+; (ΔE = 72 mV). To the best of our knowledge, the electrochemical properties of the heterocycle within **19** has not been reported and therefore we tentatively assign the signal at +0.250 V to this moiety.

The cyclic voltammograms of the Ni(II) complexes **2**, **3**, **7**, **8**, **13**, **17**, **20** and **23** revealed two irreversible reductions at −1.11 to −1.34 V and −1.63 to −1.99 V *vs.* Fc/Fc^+. Similar behaviour has been reported by Saad *et al.* for the Ni(II) complex of bis(6-benzoylthiourea-2-pyridylmethyl)(2-pyridyl methyl)amine which showed two similar irreversible reductions at −1.37 V and −1.78 V in acetonitrile.[13]

Preliminary biological antimalarial testing. Previously, the (bio)activity of thiourea ligands has been ascribed, in part, to interactions of the sulfur atom with biological substrates.[1–7] However, once coordinated to the metal centre, this group may become less accessible. Therefore we performed preliminary studies to ascertain the biological activity of some selected complexes. Affecting some 150–300 million people and causing the death of approximately 425 000 in 2015, malaria is one of the most important diseases of the developing world.[32] With concerns regarding the recent treatment failure of, and now resistance to, artemisinin combination therapies, there is an urgent demand to identify novel chemotypes to target this devastating disease. Thus, a selection of complexes was tested here, using the Malaria Sybr Green I Fluorescence assay[33] including the Ni(II), Cu(I) and Zn(II) salts of $\mathbf{L^{1a}}$, $\mathbf{L^{2a}}$ and $\mathbf{L^{3b}}$. The tabaluated results (Table 9) show the 50% Effective Concentration (EC_{50}) and the 95% Confidence Intervals (CI) for each selected compound. The EC_{50} value is therefore the concentration of compound required to inhibit growth of the intraerythrocytic asexual stage of *Plasmodium falciparum* by 50%. The biological testing results should be placed in context with previous discussion on the hydrolysis of the thiourea ligand in the zinc complexes which may not, therefore, allow a direct comparison between the different coordinated metals.

From the preliminary data it is clear that the EC_{50} values of all compounds were >1 μM, with complex **22** demonstrating the most significant activity (EC_{50} = 1.2 μM). Overall, the results suggest that the more labile d^{10} complexes of Zn(II) and Cu(I) yield more active complexes, whereas the Ni(II) variants of all ligands appear to be less potent among the series of compounds. For example, comparison of **1** *vs.* **3** and **6** *vs.* **8** shows that for a given ligand the Cu(I) species is much more active. Interestingly, comparison of **21** and **22** suggest that doubling the molar equivalents of the ligand (from 1 : 1 to 2 : 1) within the complex increases potency again alluding to the biological activity of the ligand. However, while we wished to compare these activities of the complexes against the free ligand, the low solubility of the ligand once dilituted in aqueous media meant such a comparison would not be valid. Overall, these preliminary studies suggest that in the d^{10} complexes the C=S group may be more biologically accessible *via* partial or complete dissociation of the complex suggesting an avenue for further study.

Table 9 EC_{50} values for selected complexes

Complex	EC_{50} (μM)	EC_{50} 95% CI	Complex	EC_{50} (μM)	EC_{50} 95% CI
1 (Cu)	23.3	10.2 to 15.1	10 (Zn)	6.1	4.2 to 8.9
3 (Ni)	62.5	52.6 to 74.2	21 (Cu)	14.6	7.6 to 22.3
5 (Zn)	12.4	20.8 to 26.1	22 (Cu)	1.2	0.6 to 2.4
6 (Cu)	20.5	18.8 to 22.3	23 (Ni)	12.2	10.7 to 14.0
8 (Ni)	95.1	85.7 to 105.6	24 (Zn)	14.9	12.5 to 17.8

Conclusions

In this study, six new *N*,*N*′-disubstituted thiourea derivatives ($\mathbf{L^{1a}}$–$\mathbf{L^{3b}}$) and the products resulting from their reactions with Cu(I), Cu(II), Ni(II) and Zn(II) yielded complexes (**1–24**). The synthesis and reactivity of the ligands has been explored revealing a range of metal–ligand interactions as well as varied reactivity, including controllable cleavage of ligand substituents, and heterocycle formation which can be promoted and controlled by the choice of metal ion source. X-ray crystallographic studies confirm the versatility of these ligands to form stable complexes with a range of transition metal ions. Of particular interest is the flexible binding modes of the ligand and how these are supported by commensurate H-bonding within the structure. Ease of cleavage of the acyl groups from the ligand is dependant on the metal ion co-ordinated: no cleavage was observed with Cu(II/I), where as Ni(II) facilitates cleavage at raised temperature and Zn(II) causes cleavage at room temperature. It is conceivable that ligands with such behaviour may, in future, be incorporated into metal ion sensing molecules or for thermally sensitive drug delivery devices.

Experimental

All reagents and solvents were of reagent grade quality and obtained from commercial suppliers, and used without further purification. Elemental analyses for carbon, hydrogen and nitrogen were performed on London Metropolitan University.

Magnetic susceptibilities were determined at room temperature (20 °C) using the Evans Method.[34] Electronic spectra were recorded using a Shimadzu UV-1800 UV spectrophotometer with complexes were dissolved in CH_3CN unless otherwise stated. IR spectra were carried out with a Shimadzu IR AFFINITY-1S. Electrospray mass spectroscopy (ESI-MS) was measured on a Waters LCT Premier XE (oa-TOF) mass spectrometer. The ^1H and ^{13}C NMR spectra were obtained on a Bruker AC 250 instrument using $CDCl_3$, DMSO-d^6 and acetonitrile-d^3 as solvents. Cyclic voltammetric measurements were performed using a PARSTAT potentiometer with a single compartment three-electrode cell using a platinum disk (2 mm diameter) working electrode and a platinum wire auxiliary electrode with a non aqueous $Ag/AgNO_3$ reference electrode. The ferrocene/ferrocenium couple was used as an internal reference at the end of each set of measurements. All experiments were carried out under an atmosphere of dry nitrogen. The concentration of electroactive species was approximately 1.5×10^{-3} M with tetrabutylammonium hexafluorophosphate (0.1 M) as the supporting electrolyte.

X-ray crystallography

Data collection and processing. Suitable crystals were selected and data collected following a standard method,[35] on a Rigaku AFC12 goniometer at 100 K equipped with an enhanced sensitivity (HG) Saturn724+ detector mounted at the window of an FR-E-Superbright molybdenum anode generator with either VHF Varimax optics (70 μm focus) for **1**, **15** and **21** or HF Varimax optics (100 μm focus) for **4**, **6**, **7**, **16** and **19**. Cell determination and data collection were carried out using CrystalClear.[36] With the data reduction, cell refinement and absorption correction using either CrystalClear for **1**, **6**, **7**, **16** and **19** or CrystalisPro[37] for **4**, **15** and **21**. Structure solution and refinement using SHELX programs[38] within Olex2.[39]

Antiplasmodial activity assays. *Plasmodium falciparum* $Dd2^{luc}$ were cultured using standard continuous culture conditions (RPMI1640 medium supplemented with 37.5 mM HEPES, 10 mM D-glucose, 2 mM L-glutamine, 100 μM hypoxanthine, 25 μg mL^{-1} gentamycin, 4% v/v human serum, 0.25% v/v Albumax II, 5 nM WR99210 and 2.5 μg mL^{-1} blasticidin S) at a 2% haematocrit in an atmosphere of 1% O_2, 3% CO_2, and 96% N_2. Concentration–response growth assays following exposure to tested compounds (solubilised in DMSO) were performed using the Malaria Sybr Green I Fluorescence assay as described.[33] Growth (%) normalised against an untreated control was plotted against $\log_{10}$-transformed compound concentration and the 50% Effective Concentration (EC_{50} and the 95% Confidence Intervals, CI) determined using a nonlinear regression (sigmoidal concentration–response/variable slope equation) in GraphPad Prism v5.0 (GraphPad Software, Inc., San Diego, CA).

Synthesis of the ligands

Synthesis of *N*-((5-methylpyridin-2-yl)carbamothioyl)benzamide (L^{1a}). The ligand was synthesised by a modification to a previously described method.[40] To a suspension of potassium thiocyanate (3.89 g, 40 mmol) in acetonitrile (40 cm^3) was added dropwise a solution of benzoyl chloride (5.62 g, 40 mmol) in acetonitrile (10 cm^3). The reaction mixture was heated to reflux for 3 h. After this time, the mixture was a yellow solution with a white precipitate. The mixture was filtered to remove the white KCl precipitate. The yellow solution was added to a solution of 2-amino-5-methyl pyridine (4.32 g, 40 mmol) in acetonitrile (15 cm^3) and the reaction mixture was heated to reflux for a further 15 h. The solution was left to cool and the resultant white precipitate was collected by filtration. This product was washed with acetonitrile (30 cm^3) and purified by recrystallization from chloroform : ethanol (1 : 1) to obtain white crystals (yield: 3.7 g, 85%). Melting point = 158–159 °C. ^1H NMR (250 MHz, DMSO-d^6): δ = 13.22 (1H, s, N*H*CS), 11.68 (1H, s, N*H*CO), 8.63 (1H, app. T, J_{HH} = 5.0 Hz), 8.26 (1H, s), 7.97 (2H, d, J_{HH} = 7.5 Hz), 7.72 (1H, d, J_{HH} = 5.0 Hz), 7.65 (1H, d, J_{HH} = 5.0 Hz), 7.54 (2H, app. T, J_{HH} = 7.5 Hz), 2.29 (3H, s, C*H*$_3$) ppm. $^{13}C\{^1H\}$ NMR (62.5 MHz, DMSO-d^6): δ = 177.39 (C═S), 168.48 (C═O), 148.75, 148.31, 137.95, 133.01, 131.91, 130.69, 128.58, 128.31, 115.02, 17.42 (CH_3) ppm. ESMS (*m*/*z*): 272.10 $[M + H]^+$; HRMS found *m*/*z* 272.0845, calc. 272.0858. IR (selected, cm^{-1}): 3298 (N–H), 1672 (C═O), 1333 (C═S). UV-vis. λ_{max} (ε/M^{-1} cm^{-1}): 245 (11150), 269 (15200), 316 (9200) nm.

Synthesis of *N*-((6-aminopyridin-2-yl)carbamothioyl)benzamide (L^{2a}). Using the same procedure as described for L^{1a}, but using potassium thiocyanate (3.89 g, 40 mmol), benzoyl chloride (5.62 g, 40 mmol) and 2,6-diamino pyridine (4.36 g, 40 mmol). The product was obtained as yellow crystals (yield: 3.5 g 80%). Melting point = 180–182 °C. ^1H NMR (250 MHz, DMSO-d^6): δ = 12.99 (1H, s, N*H*CS), 11.53 (1H, s, N*H*CO), 7.96 (3H, m), 7.66 (1H, app. T, J_{HH} = 7.5 Hz), 7.53 (2H, d, J_{HH} = 7.5 Hz), 7.46 (1H, d, J_{HH} = 10.0 Hz), 6.31 (1H, d, J_{HH} = 7.5 Hz), 6.14 (2H, s, N*H*$_2$) ppm. $^{13}C\{^1H\}$ NMR (62.5 MHz, DMSO-d^6): δ = 177.09 (C═S), 168.68 (C═O), 159.03, 149.54, 138.75, 133.24, 132.18, 128.77, 128.54, 106.07, 102.82 ppm. ESI-MS (*m*/*z*): 272.07 $[M]^+$; HRMS found *m*/*z* 272.0617, calc. 272.0630. IR (selected, cm^{-1}): 3485 (N–H), 3364 (N–H), 1672 (C═O), 1341 (C═S). UV-vis. λ_{max} (ε/M^{-1} cm^{-1}): 248 (14900), 278 (8050), 301 (6600), 337 (5900) nm.

Synthesis of *N*,*N*′-((pyridine-2,6-diylbis(azanediyl))bis(carbonothioyl))dibenzamide (L^{3a}). Using the same procedure as described for L^{1a}, but using potassium thiocyanate (3.89 g, 40 mmol), benzoyl chloride (5.62 g, 40 mmol) and 2,6-diamino pyridine (2.18 g, 20 mmol). The product was obtained as white crystals (yield: 2.00 g, 91%). Melting point = 197–198 °C. ^1H NMR (250 MHz, DMSO-d^6): δ = 13.15 (2H, s, N*H*CS), 11.85 (2H, s, N*H*CO), 8.53 (2H, d, J_{HH} = 5.0 Hz), 8.01 (1H, app. T, J_{HH} = 10.0 Hz), 7.98 (4H, d, J_{HH} = 7.5 Hz), 7.65 (2H, app. T, J_{HH} = 7.5 Hz), 7.53 (4H, app. T, J_{HH} = 7.5 Hz) ppm. $^{13}C\{^1H\}$ NMR (62.5 MHz, DMSO-d^6): δ = 178.47 (C═S), 168.92 (C═O), 150.18, 140.38, 133.59, 132.40, 129.13, 128.78, 113.41 ppm. ESI-MS (*m*/*z*): 436.09 $[M + H]^+$; HRMS found *m*/*z* 436.0915, calc. 436.0902. IR (selected, cm^{-1}): 3321 (N–H), 1667 (C═O), 1325 (C═S). UV-vis. λ_{max} (ε/M^{-1} cm^{-1}): 278 (19400), 331 (12200) nm.

Synthesis of *N*-((5-methylpyridin-2-yl)carbamothioyl)pival amide (L^{1b}). To a suspension of potassium thiocyanate (0.81 g, 8.3 mmol) in acetonitrile (15 cm^3) was added dropwise the solution of trimethyl acetyl chloride (1 g, 8.3 mmol) in acetonitrile (10 cm^3). The reaction mixture was heated to reflux for 3 h. The mixture was filtered to remove the white KCl precipitate. The yellow solution was then added to a solution of 2-amino-5-methyl pyridine (0.9 g, 8.3 mmol) in acetonitrile (5 cm^3) and the reaction mixture was heated to reflux for 21 h. The solution was concentrated to half of its original volume and the white precipitate of product was collected by filtration. The product was washed with cold acetonitrile (5 cm^3) and purified by recrystallization from ethanol (yield: 0.78 g, 87%). Melting point = 86–88 °C. ^{1}H NMR (250 MHz, DMSO-d^6): δ = 13.16 (1H, s, N*H*CS), 10.75 (1H, s, N*H*CO), 8.57 (1H, d, J_{HH} = 10.0 Hz), 8.25 (1H, s), 7.72 (1H, d, J_{HH} = 2.5 Hz), 2.29 (3H, s, CH_3), 1.25 (9H, s, CH_3) ppm. ^{13}C{^{1}H} NMR (100 MHz, DMSO-d^6): δ = 180.65 (C═S), 177.84 (C═O), 148.86, 148.44, 138.10, 131.00, 115.32, 40.11, 26.13 (CH_3), 17.39 (CH_3) ppm. ESI-MS (*m*/*z*): 252.08 $[M + H]^+$; HRMS found *m*/*z* 252.1169, calc. 252.1171. IR (selected, cm^{-1}): 3341 (N–H), 1676 (C═O), 1331 (C═S). UV-vis. λ_{max} (ε/M^{-1} cm^{-1}): 254 (11700), 306 (10850) nm.

Synthesis of *N*-((6-aminopyridin-2-yl)carbamothioyl)pival amide (L^{2b}). Using the same procedure as described for L^{1b}, but using potassium thiocyanate (0.81 g, 8.3 mmol), trimethyl acetyl chloride (1 g, 8.3 mmol) and 2,6-diaminopyridine (0.9 g, 8.3 mmol). The product was obtained as white crystals (yield: 0.71 g, 79%). Melting point = 164–165 °C. ^{1}H NMR (250 MHz, DMSO-d^6): δ = 12.93 (1H, s, N*H*CS), 10.58 (1H, s, N*H*CO), 7.91 (1H, d, J_{HH} = 7.5 Hz), 7.44 (1H, app. T, J_{HH} = 7.5 Hz), 6.30 (1H, d, J_{HH} = 7.5 Hz), 6.12 (2H, s, NH_2), 1.25 (9H, s, CH_3) ppm. ^{13}C{^{1}H} NMR (100 MHz, DMSO-d^6): δ = 180.34 (C═S), 176.86 (C═O), 158.83, 149.38, 138.62, 105.97, 102.51, 40.02, 26.17 (CH_3) ppm. ESI-MS (*m*/*z*): 252.08 $[M]^+$; HRMS found *m*/*z* 252.1044, calc. 252.1045. IR (selected, cm^{-1}): 3401 (N–H), 3302 (N–H), 1685 (C═O), 1356 (C═S). UV-vis. λ_{max} (ε/M^{-1} cm^{-1}): 232 (31900), 267 (17750), 292 (12850), 328 (14850) nm.

Synthesis of *N*,*N*′-((pyridine-2,6-diylbis(azanediyl))bis(carbonothioyl))bis(2,2-dimethylpropanamide) (L^{3b}). Using the same procedure as described for L^{1b}: potassium thiocyanate (1.94 g, 20 mmol), trimethyl acetyl chloride (2.4 g, 20 mmol) and 2,6-diamino pyridine (1.09 g, 10 mmol). The product was obtained as white crystals (yield: 2.00 g, 86%). Melting point = 176–177 °C. ^{1}H NMR (250 MHz, DMSO-d^6): δ = 13.19 (2H, s, N*H*CS), 10.90 (2H, s, N*H*CO), 8.53 (2H, d, J_{HH} = 7.5 Hz), 7.97 (1H, app. T, J_{HH} = 10.0 Hz), 1.26 (18H, s, CH_3) ppm. ^{13}C{^{1}H} NMR (100 MHz, DMSO-d^6): δ = 180.64 (C═S), 178.30 (C═O), 149.78, 139.99, 113.27, 40.19, 26.12 (CH_3) ppm. ESI-MS (*m*/*z*): 396.14 $[M + H]^+$; HRMS found *m*/*z* 396.1522, calc. 396.1528. IR (selected, cm^{-1}): 3445 (N–H), 3414 (N–H), 1692 (C═O), 1673 (C═O), 1366 (C═S). UV-vis. λ_{max} (ε/M^{-1} cm^{-1}): 267 (42000), 322 (47200) nm.

Synthesis of the complexes 1–24

CAUTION: Perchlorate compounds of metal ions are potentially explosive especially in presence of organic ligands. Only a small amount of material should be prepared and handled with care. All yields are calculated with respect to the moles of metal ions isolated from the reaction mixture.

Synthesis of $[Cu(L^{1a})_2]ClO_4$ (1). A solution of $Cu(ClO_4)_2{\cdot}6H_2O$ (0.185 g, 0.5 mmol) in H_2O (3 cm^3) was added to a solution of L^{1a} (0.272 g, 1.0 mmol) in DMF (4 cm^3). The mixture was stirred at room temperature for 3 h. The colourless solution turned orange and formed a precipitate. The resultant orange precipitate was filtered, washed with $CHCl_3$ (20 cm^3) to remove unreacted ligand and dried under vacuum. Red crystals of 1 were grown at room temperature by the diffusion of diethyl ether vapour into an acetonitrile solution (yield: 0.25 g, 70%). ^{1}H NMR (250 MHz, acetone-d^6): δ = 14.10 (2H, s, N*H*CS), 11.14 (2H, s, N*H*CO), 8.28 (2H, s), 8.06 (4H, d, J_{HH} = 7.5 Hz), 7.91 (2H, d, J_{HH} = 7.5 Hz), 7.72 (2H, app. T, J_{HH} = 7.5 Hz), 7.59 (4H, app. T, J_{HH} = 7.5 Hz), 7.35 (2H, app. T, J_{HH} = 10 Hz), 2.25 (6H, s, CH_3) ppm. ^{13}C NMR (62.5 MHz, acetone-d^6): δ = 170.47 (C═S), 149.49 (C═O), 148.99, 142.04, 135.03, 133.81, 132.68, 129.93, 129.65, 119.06, 111.87, 17.86 ppm. ESI-MS (*m*/*z*): 605.09 $[M - ClO_4]^+$; HRMS found *m*/*z* = 605.0854, calc. 605.0855. IR (selected, cm^{-1}): 3267 (N–H), 1672 (C═O), 1281 (C═S), 1091, 625 (Cl–O). UV-vis. λ_{max} (ε/M^{-1} cm^{-1}): 248 (24250), 268 (30600), 315 (17550) nm. Anal. Calc. For $C_{28}H_{26}ClCuN_6O_6S_2$ (%): C, 47.66; H, 3.71; N, 11.91; found (%): C, 47.58; H, 3.68; N, 11.97.

Synthesis of $[Ni(L^{1a})(L^{1c})](ClO_4)_2$ (2). $[Ni(L^{1a})(L^{1c})](ClO_4)_2$ was obtained by adding a solution of $Ni(ClO_4)_2{\cdot}6H_2O$ (0.236 g, 0.65 mmol) in methanol (5 cm^3) to a solution of L^{1a} (0.35 g, 1.3 mmol) in $CHCl_3$ (10 cm^3). The mixture was heated to reflux for 5 h. The colourless solution turned green and then a brown precipitate formed and was filtered off, washed with $CHCl_3$ (20 cm^3) to remove the unreacted ligand, and dried under vacuum to give a brown powder (yield: 0.28 g, 70%). ^{1}H NMR (250 MHz, DMSO-d^6): δ = 13.24 (1H, s, N*H*CS), 11.70 (1H, s, N*H*CS), 10.46 (2H, s, NH_2), 8.81 (1H, s, NHCO), 8.64 (1H, d, J_{HH} = 5.0 Hz), 8.27 (1H, s), 8.05 (1H, s), 7.96 (2H, d, J_{HH} = 7.5 Hz), 7.73 (1H, d, J_{HH} = 5.0 Hz), 7.66 (1H, d, J_{HH} = 7.5 Hz), 7.58 (3H, app. T, J_{HH} = 7.5 Hz), 7.05 (1H, d, J_{HH} = 7.5 Hz), 2.29 (3H, s, CH_3), 2.20 (3H, s, CH_3) ppm. ^{13}C NMR (62.5 MHz, DMSO-d^6): δ = 177.38(C═S), 168.51(C═O), 151.44, 145.31, 139.48, 133.17, 132.41, 128.68, 128.44, 127.01, 112.32, 17.37 (CH_3) ppm. ESI-MS (*m*/*z*): 495.04 $[M - 2ClO_4]^+$; HRMS found *m*/*z* 495.0575, calc. 495.0572. IR (selected, cm^{-1}): 3314 (N–H), 1672 (C═O), 1283 (C═S); 1090, 627 (Cl–O). UV-vis. λ_{max} (ε/M^{-1} cm^{-1}): 242 (15100), 272 (21500), 303 (14100), 411 (390), 584 (56) nm. Anal. Calc. For $C_{21}H_{22}Cl_2N_6NiO_9S_2$ (%): C, 36.23; H, 3.19; N, 12.07; found (%): C, 36.31; H, 3.12; N, 12.06.

Synthesis of $[Ni(L^{1a})_2](ClO_4)_2$ (3). $[Ni(L^{1a})_2](ClO_4)_2$ was obtained by stirring a mixture of $Ni(ClO_4)_2{\cdot}6H_2O$ (0.337 g, 0.92 mmol) in methanol (5 cm^3) and a solution of L^{1a} (0.5 g, 1.9 mmol) in $CHCl_3$ (10 cm^3) at 50 °C for 5 h. The colourless solution turned green and then a brown precipitate formed and was filtered off, washed with $CHCl_3$ (20 cm^3) to remove the unreacted ligand and dried under vacuum to give a brown powder (yield: 0.38 g, 52%). ^{1}H NMR (250 MHz, DMSO-d^6): δ = 13.24 (2H, s, N*H*CS), 11.71 (2H, s, N*H*CO), 8.66 (2H, app. T, J_{HH}

= 7.5 Hz), 8.27 (2H, s), 7.96 (4H, d, J_{HH} = 7.5 Hz), 7.73 (2H, d, J_{HH} = 7.5 Hz), 7.65 (2H, d, J_{HH} = 7.5 Hz), 7.55 (4H, app. T, J_{HH} = 5.0 Hz), 2.29 (6H, s, CH_3) ppm. $^{13}C\{^1H\}$ NMR (62.5 MHz, DMSO-d^6): δ = 176.08(C═S), 167.22(C═O), 157.59, 147.11, 136.76, 131.99, 127.53, 127.44, 116.26, 110.61, 16.21 (CH_3) ppm. ESI-MS (m/z): 599.01 $[M - 2ClO_4]^+$; HRMS found m/z 599.0829, calc. 599.0834. IR (selected, cm^{-1}): 3404 (N–H), 1668 (C═O), 1283 (C═S), 1087, 624 (Cl–O). UV-vis. λ_{max} (ε/M^{-1} cm^{-1}): 245 (16600), 269 (24400), 314 (12500), 394 (377), 598 (11) nm. Anal. Calc. For $C_{28}H_{26}Cl_2N_6NiO_{10}S_2$ (%): C, 42.02; H, 3.27; N, 10.50. Found (%): C, 41.95; H, 3.34; N, 10.39.

Synthesis of $[Zn(L^{1c})_2](ClO_4)_2$ (4). A methanolic solution (5 cm^3) of $Zn(ClO_4)_2{\cdot}6H_2O$ (0.28 g, 0.75 mmol) was added dropwise to a solution of L^{1a} (0.408 g, 1.5 mmol) in $CHCl_3$ (10 cm^3). The mixture was heated to reflux for 8 h. The white precipitate formed was filtered, washed with $CHCl_3$ (20 cm^3) to remove the unreacted ligand and dried under vacuum. Colourless crystals of 4 were grown at room temperature by the diffusion of diethyl ether vapour into an acetonitrile solution (yield: 0.34 g, 76%). ^{1}H NMR (250 MHz, DMSO-d^6): δ = 10.52 (2H, s, NHCS), 10.47 (2H, s, NH_2), 8.83 (2H, s, NH_2), 8.06 (2H, s), 7.60 (2H, d, J_{HH} = 10.0 Hz), 7.06 (2H, d, J_{HH} = 7.5 Hz), 2.21 (6H, s, CH_3) ppm. $^{13}C\{^1H\}$ NMR (62.5 MHz, DMSO-d^6): δ = 180.44 (C═S), 151.78, 145.47, 139.84, 126.59, 112.84, 17.37 (CH_3) ppm. ESI-MS (m/z): 397.05 $[M - 2ClO_4]^+$; HRMS found m/z 397.0230, calc. 397.0248. IR (selected, cm^{-1}): 3381 (N–H), 1279 (C═S), 1080, 626 (Cl–O). UV-vis. λ_{max} (ε/M^{-1} cm^{-1}): 240 (14900), 273 (28450), 299 (25600) nm. Anal. Calc. For $C_{14}H_{18}Cl_2N_6O_8S_2Zn$ (%): C, 28.09; H, 3.03; N, 14.04; found (%): C, 28.16; H, 3.01; N, 14.12.

This product was also obtained *via* the same procedure as described for 4 but using $Zn(ClO_4)_2{\cdot}6H_2O$ (0.22 g, 0.6 mmol) and L^{1b} (0.3 g, 1.2 mmol). The product was isolated as a white powder (yield: 0.2 g, 69%).

Synthesis of $[Zn(L^{1a})(L^{1c})](ClO_4)_2$ (5). A methanolic solution (5 cm^3) of $Zn(ClO_4)_2{\cdot}6H_2O$ (0.34 g, 0.92 mmol) was added dropwise to a solution of L^{1a} (0.5 g, 1.84 mmol) in $CHCl_3$ (10 cm^3). The mixture was stirred at room temperature for 8 h. The white precipitate formed was filtered, washed with $CHCl_3$ (20 cm^3) to remove the unreacted ligand and dried under vacuum (yield: 0.36 g, 56%). ^{1}H NMR (250 MHz, DMSO-d^6): δ = 10.52 (1H, s, NHCS), 10.46 (1H, s, NHCS), 8.82 (1H, s, NHCO), 8.05 (2H, s), 7.95 (2H, d, J_{HH} = 7.5 Hz), 7.65 (1H, app. t, J_{HH} = 7.5 Hz), 7.60 (1H, d, J_{HH} = 2.5 Hz), 7.57 (1H, d, J_{HH} = 2.5 Hz), 7.52 (2H, app. t, J_{HH} = 7.5 Hz), 7.05 (2H, d, J_{HH} = 7.5 Hz), 4.01 (2H, s, NH_2), 2.20 (6H, s, CH_3) ppm. ^{13}C NMR (62.5 MHz, DMSO-d^6): δ = 180.35 (C═S), 166.30(C═O), 151.65, 145.53, 139.77, 133.47, 129.71, 129.25, 128.92, 127.14, 112.43, 17.33 ppm. ESI-MS (m/z): 501.00 $[M - H - 2ClO_4]$; HRMS found m/z = 501.0331, calc. 501.0339. IR (selected, cm^{-1}): 3377 (N–H), 1670 (C═O), 1278 (C═S), 1084, 627 (Cl–O). UV-vis. λ_{max} (ε/M^{-1} cm^{-1}): 235 (24300), 273 (33950), 299 (29800) nm. Anal. Calc. For $C_{21}H_{22}Cl_2N_6O_9S_2Zn$ (%): C, 35.89; H, 3.16; N, 11.96; found (%): C, 35.72; H, 2.88; N, 11.82.

Synthesis of $[Cu(L^{2a})_2]ClO_4$ (6). Using the same procedure as described for **1**, but using $Cu(ClO_4)_2{\cdot}6H_2O$ (0.4 g, 1.1 mmol), L^{2a} (0.589 g, 2.2 mmol). Dark orange crystals of **6** were grown at room temperature by the diffusion of diethyl ether vapour into an acetonitrile : methanol (2 : 1) solution of it (yield: 0.51 g, 66%). ^{1}H NMR (250 MHz, CD_3CN): δ = 13.23 (2H, s, NHCS), 9.68 (2H, s, NHCO), 7.91 (4H, d, J_{HH} = 7.5 Hz), 7.69 (2H, app. t, J_{HH} = 7.5 Hz), 7.55 (6H, app. t, J_{HH} = 7.5 Hz), 7.34 (2H, d, J_{HH} = 10.0 Hz), 6.49 (2H, d, J_{HH} = 7.5 Hz), 5.29 (4H, s, NH_2) ppm. $^{13}C\{^1H\}$ NMR (62.5 MHz, CD_3CN): δ = 174.72 (C═S), 168.88 (C═O), 158.06, 149.87, 140.22, 133.52, 132.61, 128.68, 128.59, 103.07, 100.66 ppm. ESI-MS (m/z): 607.08 $[M - ClO_4]^+$; HRMS found m/z = 607.0754, calc. 607.0760. IR (selected, cm^{-1}): 3323 (N–H), 1661 (C═O), 1258 (C═S), 1080, 624 (Cl–O). UV-vis. λ_{max} (ε/M^{-1} cm^{-1}): 247 (33650), 279 (18200), 302 (14700), 344 (12850) nm. Anal. Calc. For $C_{26}H_{24}ClCuN_8O_6S_2$ (%): C, 44.13; H, 3.42; N, 15.84; found (%): C, 44.04; H, 3.47; N, 15.72.

Synthesis of $[Ni(L^{2c})_2](ClO_4)_2$ (7). $[Ni(L^{2c})_2](ClO_4)_2$ was obtained by using the same procedure as described for **2**, using $[Ni(ClO_4)_2].6H_2O$ (0.2 g, 0.55 mmol) and L^{2a} (0.3 g, 1.1 mmol). Red crystals of **7** were grown at room temperature by the diffusion of diethyl ether vapour into an ethyl acetate solution (yield: 0.21 g, 64%). ^{1}H NMR (250 MHz, DMSO-d^6): δ = 10.61 (2H, s, NHCS), 10.05 (2H, s, NH_2), 8.66 (2H, s, NH_2), 7.28 (2H, app. t, J_{HH} = 7.5 Hz), 6.20 (6H, m), 6.00 (2H, d, J_{HH} = 7.5 Hz) ppm. $^{13}C\{^1H\}$ NMR (62.5 MHz, DMSO-d^6): δ = 179.99 (C═S), 157.50, 139.08, 129.08, 128.78, 100.98, 98.88 ppm. ESI-MS (m/z): 393.02 $[M - H - 2ClO_4]^+$; HRMS found m/z = 393.0206, calc. 393.0215. IR (selected, cm^{-1}): 3343 (N–H), 1271 (C═S), 1071, 627 (Cl–O). UV-vis. λ_{max} (ε/M^{-1} cm^{-1}): 215 (16900), 251 (20050), 272 (18950), 319 (22950), 401 (205), 603 (17) nm. Anal. Calc. For $C_{12}H_{16}Cl_2N_8NiO_8S_2$ (%): C, 24.26; H, 2.72; N, 18.86; found (%): C, 24.20; H, 2.83; N, 18.79.

This product was also obtained *via* the same procedure described for **2**, but with $[Ni(ClO_4)_2].6H_2O$ (0.25 g, 0.69 mmol) and L^{2b} (0.35 g, 1.4 mmol). The product was isolated as a brown powder (yield: 0.24 g, 69%).

Synthesis of $[Ni(L^{2a})_2](ClO_4)_2$ (8). $[Ni(L^{2a})_2](ClO_4)_2$ was obtained as a brown powder by using the same procedure as described for **3**, but using $Ni(ClO_4)_2{\cdot}6H_2O$ (0.336 g, 0.92 mmol) and L^{2a} (0.5 g, 1.84 mmol). The product was isolated as a brown powder (yield: 0.34 g, 46%). ^{1}H NMR (250 MHz, DMSO-d^6): δ = 13.00 (2H, s, NHCS), 11.55 (2H, s, NHCO), 7.95 (4H, d, J_{HH} = 5.0 Hz), 7.64 (4H, d, J_{HH} = 5.0 Hz), 7.52 (4H, app. t, J_{HH} = 7.5 Hz), 7.28 (2H, app. t, J_{HH} = 7.0 Hz), 6.21 (4H, s, NH_2), 6.18 (2H, app. t, J_{HH} = 10.0 Hz) ppm. $^{13}C\{^1H\}$ NMR (62.5 MHz, DMSO-d^6): δ = 176.09 (C═S), 165.60 (C═O), 158.36, 156.75, 138.90, 132.87, 132.77, 128.33, 128.04, 109.43, 105.80 ppm. ESI-MS (m/z): 601.08 $[M - H - 2ClO_4]^+$; HRMS found m/z = 601.0742, calc. 601.0739. IR (selected, cm^{-1}): 3331 (N–H), 1660 (C═O), 1275 (C═S), 1071, 626 (Cl–O). UV-vis. λ_{max} (ε/M^{-1} cm^{-1}): 235 (16550), 250 (19300), 273 (13550), 324 (11500), 421 (423), 612 (5) nm. Anal. Calc. For $C_{26}H_{24}Cl_2N_8NiO_{10}S_2$ (%): C, 38.93; H, 3.02; N, 13.97; found (%): C, 38.87; H, 3.13; N, 13.92.

Synthesis of $[Zn(L^{2c})_2](ClO_4)_2$ (9). Using the same procedure as described for **4**, using $Zn(ClO_4)_2{\cdot}6H_2O$ (0.24 g, 0.64 mmol)

and $\mathbf{L^{2a}}$ (0.35 g, 1.3 mmol). The product was isolated as a white powder (yield: (0.28 g, 73%). ^{1}H NMR (400 MHz, DMSO-d^6): δ = 10.63 (2H, s, N*H*CS), 10.06 (2H, s, NH_2), 8.68 (2H, s, NH_2), 7.29 (2H, app. t, J_{HH} = 2.5 Hz), 6.22 (6H, m), 6.02 (2H, d, J_{HH} = 5.0 Hz) ppm. ^{13}C{^{1}H} NMR (100 MHz, DMSO-d^6): δ = 180.05 (C═S), 157.74, 152.40, 139.39, 101.00, 98.79 ppm. ESI-MS (*m*/*z*): 399.00 [M − H − 2ClO$_4$]$^+$; HRMS found *m*/*z* 399.0000, calc. 399.0000. IR (selected, cm^{-1}): 3375 (N–H), 1267 (C═S), 1067 (Cl–O), 626 (Cl–O). UV-vis. λ_{max} (ε/M^{-1} cm^{-1}): 214 (28200), 251 (34100), 272 (31750), 320 (38250) nm. Anal. Calc. For $C_{12}H_{16}Cl_2N_8O_8S_2Zn$ (%): C, 23.99; H, 2.68; N, 18.65; found (%): C, 24.13; H, 2.73; N, 18.48.

This product was also obtained as described for **4** but using Zn(ClO$_4$)$_2$·6H$_2$O (0.25 g, 0.67 mmol) and $\mathbf{L^{2b}}$ (0.34 g, 1.3 mmol). The product was isolated as a white powder (yield: 0.27 g, 81%).

Synthesis of [Zn(L^{2a})(L^{2c})](ClO$_4$)$_2$ (10). Using the same procedure as described for **5** but using Zn(ClO$_4$)$_2$·6H$_2$O (0.17 g, 0.46 mmol) was added dropwise to a solution of $\mathbf{L^{2a}}$ (0.25 g, 0.92 mmol). The product was isolated as a white powder (yield: 0.18 g, 57%). ^{1}H NMR (250 MHz, DMSO-d^6): δ = 10.62 (2H, s, N*H*CS), 10.06 (1H, s, N*H*CO), 8.67 (2H, s, NH_2), 7.95 (2H, d, J_{HH} = 7.5 Hz), 7.66 (1H, app. t, J_{HH} = 7.5 Hz), 7.52 (2H, app. t, J_{HH} = 7.5 Hz), 7.29 (2H, app. t, J_{HH} = 7.5 Hz), 6.19 (2H, d, J_{HH} = 7.5 Hz), 6.02 (2H, d, J_{HH} = 7.5 Hz), 3.85 (4H, s, NH_2) ppm. ^{13}C{^{1}H} NMR (62.5 MHz, DMSO-d^6): δ = 180.35 (C═S), 166.26 (C═O), 157.86, 152.35, 139.55, 133.48, 129.65, 129.25, 128.93, 101.20, 98.79 ppm. ESI-MS (*m*/*z*): 504.05 [M − H − 2ClO$_4$]$^+$; HRMS found *m*/*z* 504.0663, calc. 504.0674. IR (selected, cm^{-1}): 3366 (N–H), 1668 (C═O), 1277 (C═S), 1070 (Cl–O), 626 (Cl–O). UV-vis. λ_{max} (ε/M^{-1} cm^{-1}): 222 (21100), 275 (14000), 326 (8150), 367 (10300) nm. Anal. Calc. For $C_{19}H_{20}Cl_2N_8O_9S_2Zn$ (%): C, 32.38; H, 2.86; N, 15.90; found (%): C, 32.40; H, 3.14; N, 15.84.

Synthesis of [Cu(L^{3a})]ClO$_4$ (11). Using the same procedure as described for **1**, but using Cu(ClO$_4$)$_2$·6H$_2$O (0.21 g, 0.57 mmol) and $\mathbf{L^{3a}}$ (0.25 g, 0.57 mmol). The product was isolated as a brown powder (yield: 0.16 g, 47%). ^{1}H NMR (250 MHz, DMSO-d^6): δ = 12.14 (2H, s, N*H*CS), 11.74 (2H, s, N*H*CO), 8.25 (2H, d, J_{HH} = 7.5 Hz), 8.11 (2H, d, J_{HH} = 7.5 Hz), 7.93 (1H, d, J_{HH} = 7.5 Hz), 7.69 (1H, app. t, J_{HH} = 7.5 Hz), 7.59 (7H, m) ppm. ^{13}C{^{1}H} NMR (62.5 MHz, DMSO-d^6): δ = 176.50 (C═S), 169.51 (C═O), 150.24, 140.39, 133.53, 132.77, 132.27, 131.50, 128.66, 128.59, 113.19, 107.09 ppm. ESI-MS (*m*/*z*): 498.02 [M − ClO$_4$]$^+$; HRMS found *m*/*z* 498.0110, calc. 498.0120. IR (selected, cm^{-1}): 3387 (N–H), 1665 (C═O), 1260 (C═S), 1096 (Cl–O), 621 (Cl–O). UV-visible λ_{max} (ε/M^{-1} cm^{-1}): 263 (23200), 316 (18400), 359 (19400) nm. Anal. Calc. For $C_{21}H_{17}ClCuN_5O_6S_2$ (%): C, 42.14; H, 2.86; N, 11.70; found (%): C, 42.30; H, 3.00; N, 11.69.

Synthesis of [Cu(L^{3a})$_2$] ClO$_4$ (12). Using the same procedure as described for **1** but using Cu(ClO$_4$)$_2$·6H$_2$O (0.106 g, 0.29 mmol) and $\mathbf{L^{3a}}$ (0.25 g, 0.57 mmol). The product was isolated as an orange powder (yield: 0.17 g, 57%). ^{1}H NMR (250 MHz, DMSO-d^6): δ = 12.15 (4H, s, N*H*CS), 11.73 (4H, s, N*H*CO), 8.23 (8H, d, J_{HH} = 2.5 Hz), 8.14 (2H, app. t, J_{HH} = 5.0 Hz), 8.02 (4H, d, J_{HH} = 5.0 Hz), 7.64 (4H, app. t, J_{HH} = 5.0 Hz), 7.56 (8H, J_{HH} = 5.0 Hz) ppm. ^{13}C{^{1}H} NMR (62.5 MHz, DMSO-d^6): δ = 176.42 (C═S), 168.78 (C═O), 162.32, 141.10, 133.58, 132.20, 129.05, 128.67, 114.61 ppm. ESI-MS (*m*/*z*): 933.09 [M − H − ClO$_4$]$^+$; HRMS found *m*/*z* 933.1029, calc. 933.1045. IR (selected, cm^{-1}): 3340 (N–H), 1667 (C═O), 1252 (C═S), 1096 (Cl–O), 621 (Cl–O). UV-visible λ_{max} (ε/M^{-1} cm^{-1}): 268 (40950), 336 (24600) nm. Anal. Calc. For $C_{42}H_{34}ClCuN_{10}O_8S_4$ (%): C, 48.79; H, 3.31; N, 13.55; found (%): C, 48.46; H, 2.92; N, 13.47.

Synthesis of [Ni(L^{3a})$_2$](ClO$_4$)$_2$ (13). Obtained using the same procedure as described for **3**, but with Ni(ClO$_4$)$_2$·6H$_2$O (0.11 g, 0.29 mmol) and $\mathbf{L^{3a}}$ (0.25 g, 0.57 mmol). The product was isolated as a green powder (yield: 0.17 g, 50%). ESI-MS (*m*/*z*): 928.10 [M − 2ClO$_4$]$^+$; HRMS found *m*/*z* 928.2207, calc. 928.2233. IR (selected, cm^{-1}): 3469 (N–H), 1663 (C═O), 1277 (C═S), 1064 (Cl–O), 627 (Cl–O). UV-vis. λ_{max} (ε/M^{-1} cm^{-1}): 281 (24300), 331 (14200), 413 (212), 583 (21), 936 (12) nm. Anal. Calc. For $C_{42}H_{34}Cl_2N_{10}NiO_{12}S_4$ (%): C, 44.70; H, 3.04; N, 12.41; found (%): C, 44.67; H, 2.68; N, 12.39.

Synthesis of [Zn(L^{3a})$_2$](ClO$_4$)$_2$ (14). Using the same procedure as described for **5** but using [Zn(ClO$_4$)$_2$]·6H$_2$O (0.214 g, 0.57 mmol) and $\mathbf{L^{3a}}$ (0.5 g, 1.1 mmol). The product was isolated as a white powder (yield: 0.32 g, 49%). ^{1}H NMR (250 MHz, DMSO-d^6): δ = 12.86 (2H, s, N*H*CS), 11.67 (2H, s, N*H*CS), 10.61 (2H, s, N*H*CO), 10.05 (2H, s, NH_2), 9.00 (2H, s, NH_2), 7.94–7.99 (4H, m), 7.84 (4H, d, J_{HH} = 7.5 Hz), 7.66 (4H, app. t, J_{HH} = 7.5 Hz), 7.44 (2H, d, J_{HH} = 7.5 Hz), 7.02 (2H, d, J_{HH} = 10.0 Hz) ppm. ^{13}C{^{1}H} NMR (62.5 MHz, DMSO-d^6): δ = 180.23 (C═S), 178.09 (C═S), 168.13 (C═O), 152.04, 148.35, 140.66, 133.51, 132.27, 128.94, 128.65, 109.97, 109.76 ppm. IR (selected, cm^{-1}): 3318 (N–H), 1664 (C═O), 1273 (C═S), 1095 (Cl–O), 627 (Cl–O). UV-vis. λ_{max} (ε/M^{-1} cm^{-1}): 281 (29900), 326 (20800) nm. Anal. Calc. For $C_{28}H_{26}Cl_2N_{10}O_{10}S_4Zn$ (%): C, 36.28; H, 2.83; N, 15.11; found (%): C, 35.90; H, 2.66; N, 14.95.

Synthesis of [Cu(L^{1b})$_2$](ClO$_4$) (15). As described for **1** but using Cu(ClO$_4$)$_2$·6H$_2$O (0.22 g, 0.59 mmol) and $\mathbf{L^{1b}}$ (0.298 g, 1.2 mmol). Orange crystals of **15** were grown at room temperature by the diffusion of diethyl ether vapour into a $CHCl_3$ solution (yield: 0.20 g, 51%). ^{1}H NMR (400 MHz, CD_3CN): δ = 13.60 (2H, s, N*H*CS), 9.09 (2H, s, N*H*CO), 8.15 (2H, s), 7.75 (2H, d, J_{HH} = 5.0 Hz), 7.45 (2H, d, J_{HH} = 5.0 Hz), 2.29 (6H, s, CH_3), 1.29 (18H, s, CH_3) ppm. ^{13}C{^{1}H} NMR (100 MHz, CD_3CN): δ = 182.39 (C═S), 176.90 (C═O), 149.41, 148.51, 141.72, 133.93, 118.97, 41.21, 26.36 (CH_3), 18.19 (CH_3) ppm. ESI-MS (*m*/*z*): 565.15 [M − ClO$_4$]$^+$; HRMS found *m*/*z* 565.1470, calc. 565.1481. IR (selected, cm^{-1}): 3358 (N–H), 1676 (C═O), 1283 (C═S), 1096 (Cl–O), 621 (Cl–O). UV-vis. λ_{max} (ε/M^{-1} cm^{-1}): 254 (23900), 307 (22000) nm. Anal. Calc. For $C_{24}H_{34}ClCuN_6O_6S_2$ (%): C, 43.30; H, 5.15; N, 12.62; found (%): C, 43.34; H, 5.06; N, 12.57.

Synthesis of [Cu(L^{1b})Cl] (16). A solution of $\mathbf{L^{1b}}$ (0.30 g, 1.2 mmol) in $CHCl_3$ (4 cm^3) was added to a solution of $CuCl_2$·2H$_2$O (0.10 g, 0.6 mmol) in methanol (4 cm^3). The mixture was stirred for 4 h at room temperature. The colourless solution turned orange with a precipitate. The orange precipitate formed was filtered, washed with $CHCl_3$ (20 cm^3) to

remove unreacted ligand, and dried under vacuum. Red crystals of **16** were grown at room temperature by the diffusion of diethyl ether vapour into a chloroform solution (yield: 0.26 g, 78%). ^{1}H NMR (400 MHz, $CDCl_3$): δ = 13.73 (1H, s, N*H*CS), 9.67 (1H, s, N*H*CO), 8.50 (1H, s), 7.67 (1H, d, J_{HH} = 5.0 Hz), 7.17 (1H, d, J_{HH} = 5.0 Hz), 2.38 (3H, s, CH_3), 1.43 (9H, s, CH_3) ppm. ^{13}C{^{1}H} NMR (125 MHz, $CDCl_3$): δ = 181.94 (C═S), 174.69 (C═O), 149.19, 146.70, 140.06, 132.60, 117.88, 40.96, 26.65, 17.95 ppm. ESI-MS (*m*/*z*): 371.13 $[M + Na]^+$. IR (selected, cm^{-1}): 3450 (N–H), 1673 (C═O), 1275 (C═S). UV-vis. λ_{max} (ε/M^{-1} cm^{-1}): 293 (9500), 318 (7600) nm. Anal. Calc. For $C_{12}H_{17}ClCuN_3OS$ (%): C, 41.14; H, 4.89; N, 11.99; found (%): C, 40.94; H, 4.65; N, 12.04.

Synthesis of $[Ni(L^{1b})_2](ClO_4)_2$ (17). Obtained using the same procedure as described for **3**, but with $Ni(ClO_4)_2{\cdot}6H_2O$ (0.255 g, 0.7 mmol) and $\mathbf{L^{1b}}$ (0.35 g, 1.4 mmol). The product was isolated as a brown powder (yield: 0.27 g, 51%). ^{1}H NMR (250 MHz, DMSO-d^6): δ = 13.15 (2H, s, N*H*CS), 10.74 (2H, s, N*H*CO), 8.56 (2H, d, J_{HH} = 5.0 Hz), 8.23 (2H, s), 7.69 (2H, d, J_{HH} = 10.0 Hz), 2.27 (6H, s, CH_3), 1.24 (18H, s, CH_3) ppm. ^{13}C{^{1}H} NMR (62.5 MHz, DMSO-d^6): δ = 177.23 (C═S), 174.83 (C═O), 161.21, 147.56, 137.53, 125.84, 114.22, 40.00, 25.52 (CH_3), 17.02 (CH_3) ppm. ESI-MS (*m*/*z*): 559.15 $[M - H - 2ClO_4]^+$; HRMS found *m*/*z* 559.1451, calc. 559.1460. IR (selected, cm^{-1}): 3321 (N–H), 1675 (C═O), 1287 (C═S), 1092 (Cl–O), 626 (Cl–O). UV-vis. λ_{max} (ε/M^{-1} cm^{-1}): 257 (9100), 304 (9250), 390 (329), 597 (11) nm. Anal. Calc. For $C_{24}H_{34}Cl_2N_6NiO_{10}S_2$ (%): C, 37.92; H, 4.51; N, 11.05; found (%): C, 37.80; H, 4.58; N, 10.97.

Synthesis of $[Cu(L^{2b})_2](ClO_4)$ (18). The same procedure as described for **1** but using $Cu(ClO_4)_2{\cdot}6H_2O$ (0.26 g, 0.69 mmol) and $\mathbf{L^{2b}}$ (0.35 g, 1.4 mmol). The product was isolated as a brown powder (yield: 0.29 g, 63%). ^{1}H NMR (250 MHz, CD_3CN): δ = 13.25 (2H, s, N*H*CS), 8.94 (2H, s, N*H*CO), 7.54 (2H, app. T, J_{HH} = 7.5 Hz), 7.01 (2H, d, J_{HH} = 7.5 Hz), 6.50 (2H, d, J_{HH} = 10.0 Hz), 5.37 (4H, s, NH_2), 1.26 (18H, s, CH_3) ppm. ^{13}C{^{1}H} NMR (62.5 MHz, CD_3CN): δ = 182.51 (C═S), 176.62 (C═O), 159.48, 149.07, 141.61, 41.38, 27.18 (CH_3) ppm. ESI-MS (*m*/*z*): 567.20 $[M - ClO_4]^+$; HRMS found *m*/*z* 567.1367, calc. 567.1386. IR (selected, cm^{-1}): 3343 (N–H), 1671 (C═O), 1267 (C═S), 1079 (Cl–O), 625 (Cl–O). UV-vis. λ_{max} (ε/M^{-1} cm^{-1}): 230 (12000), 268 (6400), 296 (4300), 332 (5650) nm. Anal. Calc. For $C_{22}H_{32}ClCuN_8O_6S_2$ (%): C, 39.58; H, 4.83; N, 16.78; found (%): C, 39.37; H, 4.70; N, 16.46.

Synthesis of $[Cu(L^4)_2Cl_2]$ (19). A solution of $CuCl_2{\cdot}6H_2O$ (0.1 g, 0.59 mmol) in methanol (4 cm^3) was added to a solution of $\mathbf{L^{2b}}$ (0.3 g, 1.2 mmol) in $CHCl_3$ (8 cm^3). The mixture was stirred for 3 h at room temperature. The colourless solution turned orange with a precipitate. The orange precipitate was collected by filtration, washed with $CHCl_3$ (20 cm^3) to remove unreacted ligand, and dried under vacuum. Dark orange crystals of **19** were grown at room temperature by the diffusion of diethyl ether vapour into a DCM : ethanol (1 : 1) solution of the product (yield: 0.18 g, 48%). ESI-MS (*m*/*z*): 667.04 $[M + MeOH]^+$. IR (selected, cm^{-1}): 3320 (N–H), 1683 (C═O), 1273 (C═S). UV-vis. λ_{max} (ε/M^{-1} cm^{-1}): 264 (26900), 282 (22800), 326 (22100), 470 (139) nm. Anal. Calc. For $C_{22}H_{28}Cl_2CuN_8O_2S_2$ (%): C, 41.61; H, 4.44; N, 17.64; found (%): C, 41.28; H, 4.43; N, 17.25.

Synthesis of $[Ni(L^{2b})_2](ClO_4)_2$ (20). Obtained using the same procedure described for **3**, but with $Ni(ClO_4)_2{\cdot}6H_2O$ (0.36 g, 1 mmol) and $\mathbf{L^{2b}}$ (0.5 g, 2 mmol). The product was isolated as a brown powder (yield: 0.38 g, 51%). ^{1}H NMR (250 MHz, DMSO-d^6): δ = 12.91 (2H, s, N*H*CS), 10.56 (2H, s, N*H*CO), 7.88 (2H, d, J_{HH} = 7.5 Hz), 7.42 (2H, app. t, J_{HH} = 7.5 Hz), 6.28 (2H, d, J_{HH} = 7.5 Hz), 6.10 (4H, s, NH_2), 1.22 (18H, s, CH_3) ppm. ^{13}C{^{1}H} NMR (62.5 MHz, DMSO-d^6): δ = 179.81 (C═S), 176.03 (C═O), 158.53, 148.85, 138.08, 105.48, 102.15, 30.37, 25.81 (CH_3) ppm. ESI-MS (*m*/*z*): 561.09 $[M - 2ClO_4]^+$; HRMS found *m*/*z* 561.1377, calc. 561.1365. IR (selected, cm^{-1}): 3377 (N–H), 1664 (C═O), 1277 (C═S), 1071 (Cl–O), 627 (Cl–O). UV-vis. λ_{max} (ε/M^{-1} cm^{-1}): 232 (41600), 268 (24100), 294 (15500), 328 (21550), 410 (340), 606 (7) nm. Anal. Calc. For $C_{22}H_{32}Cl_2N_8NiO_{10}S_2$ (%): C, 34.67; H, 4.23; N, 14.70; found (%): C, 34.58; H, 4.29; N, 14.72.

Synthesis of $[Cu(L^{3b})]ClO_4$ (21). Using the same procedure as described for **1** but using $Cu(ClO_4)_2{\cdot}6H_2O$ (0.328 g, 0.89 mmol) and $\mathbf{L^{3b}}$ (0.35 g, 0.89 mmol). Yellow crystals of **21** were grown at room temperature by the diffusion of diethyl ether vapour into an ethanol : DCM (3 : 1) solution of the product (yield: 0.28 g, 56%). ^{1}H NMR (250 MHz, DMSO-d^6): δ = 11.99 (2H, s, N*H*CS), 11.00 (2H, s, N*H*CO), 8.17 (1H, app. t, J_{HH} = 7.5 Hz), 7.94 (1H, d, J_{HH} = 7.5 Hz), 7.64 (1H, d, J_{HH} = 7.5 Hz), 1.29 (18H, s, CH_3) ppm. ^{13}C{^{1}H} NMR (62.5 MHz, DMSO-d^6): δ = 187.38 (C═S), 181.39 (C═O), 149.85, 140.40, 139.85, 112.84, 107.67, 26.23 (CH_3), 25.84, 25.32 (CH_3), 24.96 ppm. ESI-MS (*m*/*z*): 458.06 $[M - ClO_4]^+$; HRMS found *m*/*z* 458.0869, calc. 458.0871. IR (selected, cm^{-1}): 3400 (N–H), 1688 (C═O), 1277 (C═S), 1090 (Cl–O), 625 (Cl–O). UV-vis. λ_{max} (ε/M^{-1} cm^{-1}): 298 (6650), 350 (6500) nm. Anal. Calc. For $C_{17}H_{25}ClCuN_5O_6S_2$ (%): C, 36.56; H, 4.51; N, 12.54; found (%): C, 36.31; H, 4.41; N, 12.68.

Synthesis of $[Cu(L^{3b})_2]ClO_4$ (22). Using the same procedure as described for **1** but using $Cu(ClO_4)_2{\cdot}6H_2O$ (0.164 g, 0.44 mmol) and $\mathbf{L^{3b}}$ (0.35 g, 0.89 mmol). The product was isolated as a brown powder (yield: 0.23 g, 55%). ^{1}H NMR (250 MHz, CD_3CN): δ = 13.64 (4H, s, N*H*CS), 9.18 (4H, s, N*H*CO), 7.99 (2H, app. t, J_{HH} = 7.5 Hz), 7.73 (4H, d, J_{HH} = 10.0 Hz), 1.29 (36H, s, CH_3) ppm. ^{13}C{^{1}H} NMR (62.5 MHz, CD_3CN): δ = 182.79 (C═S), 178.32 (C═O), 149.38, 143.13, 117.19, 41.85, 26.96 (CH_3) ppm. ESI-MS (*m*/*z*): 853.22 $[M - ClO_4]^+$; HRMS found *m*/*z* 853.2182, calc. 853.2195. IR (selected, cm^{-1}): 3397 (N–H), 1690 (C═O), 1277 (C═S), 1077 (Cl–O), 624 (Cl–O). UV-vis. λ_{max} (ε/M^{-1} cm^{-1}): 278 (20700), 290 (20750), 326 (14800) nm. Anal. Calc. For $C_{34}H_{50}ClCuN_{10}O_8S_4$ (%): C, 42.80; H, 5.28; N, 14.68; found (%): C, 42.46; H, 4.93; N, 14.63.

Synthesis of $[Ni(L^{3b})_2](ClO_4)_2$ (23). Obtained using the same procedure described for **3**, but using $Ni(ClO_4)_2{\cdot}6H_2O$ (0.14 g, 0.38 mmol) and $\mathbf{L^{3b}}$ (0.3 g, 0.76 mmol). The product was isolated as a green powder (yield: 0.20 g, 50%). ESI-MS (*m*/*z*): 847.25 $[M - 2ClO_4]^+$; HRMS found *m*/*z* 847.2164; calc. 847.2175. IR (selected, cm^{-1}): 3312 (N–H), 1687 (C═O), 1262 (C═S), 1090 (Cl–O), 626 (Cl–O). UV-vis. λ_{max} (ε/M^{-1} cm^{-1}): 267 (38800), 323 (39050), 421 (242), 591 (5), 952 (3) nm. Anal. Calc.

For $C_{34}H_{50}Cl_2N_{10}NiO_{12}S_4$ (%): C, 38.94; H, 4.81; N, 13.36; found (%): C, 39.10; H, 4.72; N, 13.46.

Synthesis of $[Zn(L^{3c'})_2](ClO_4)_2$ (24). Using the same procedure described for **4**, but using $Zn(ClO_4)_2{\cdot}6H_2O$ (0.165 g, 0.44 mmol) and L^{3b} (0.35 g, 0.89 mmol). The product was isolated as a white powder (yield: 0.26 g, 67%). ^{1}H NMR (250 MHz, CD_3CN): δ = 12.93 (2H, s, N*H*CS), 10.77 (2H, s, N*H*CS), 10.60 (2H, s, N*H*CS), 10.00 (2H, s, N*H*CS), 8.99 (2H, s, N*H*CO), 7.91 (2H, d, J_{HH} = 7.5 Hz), 7.82 (2H, t, J_{HH} = 10.0 Hz), 7.01 (2H, d, J_{HH} = 10.0 Hz), 1.25 (18H, s, CH_3) ppm. $^{13}C\{^1H\}$ NMR (62.5 MHz, CD_3CN): δ = 180.39, 180.23 (C═S), 178.28 (C═O), 151.88, 150.30, 148.22, 140.66, 110.09, 40.27, 26.30 (CH_3) ppm. ESI-MS (m/z): 685.09 $[M - 2ClO_4]^+$; HRMS found m/z 685.0972; calc. 685.0962. IR (selected, cm^{-1}): 3317 (N–H), 1689 (C═O), 1258 (C═S), 1075 (Cl–O), 626 (Cl–O). UV-vis. λ_{max} (ε/M^{-1} cm^{-1}): 282 (27500), 326 (21200) nm. Anal. Calc. For $C_{24}H_{34}Cl_2N_{10}O_{10}S_4Zn$ (%): C, 32.49; H, 3.86; N, 15.79; found (%): C, 32.28; H, 3.54; N, 15.54.

Conflicts of interest

There are no conflicts to declare.

Acknowledgements

We thank the Iraqi Ministry of Higher Education and Scientific Research for funding (A. A. A. A) and Basrah University for support. Cardiff University are also thanked for support. Mr Christopher Barker (Keele University) is thanked for collection of antimalarial data. The staff of the EPSRC National Mass Spectrometry Service at Swansea University and EPSRC National Crystallographic Service at the University of Southampton are also thanked.

Notes and references

1 J.-F. Zhang, J.-Y. Xu, B.-L. Wang, Y.-X. Li, L.-X. Xiong, Y.-Q. Li, Y. Ma and Z.-M. Li, *J. Agric. Food Chem.*, 2012, **60**, 7565–7572; B.-L. Wang, H.-W. Zhu, Y. Ma, L.-X. Xiong, Y.-Q. Li, Y. Zhao, J.-F. Zhang, Y.-W. Chen, S. Zhou and Z.-M. Li, *J. Agric. Food Chem.*, 2013, **61**, 5483–5493.

2 M. K. Rauf, A. Imtaiz-ud-Din, A. Badshah, M. Gielen, M. Ebihara, D. De Vos and S. Ahmed, *J. Inorg. Biochem.*, 2009, **103**, 1135–1144.

3 S. Cunha, F. C. Macedo Jr., G. A. N. Costa, M. T. Rodrigues Jr., R. B. V. Verde, L. C. de Souza Neta, I. Vencato, C. Lariucci and F. P. Sá, *Monatsh. Chem.*, 2007, **138**, 511–516.

4 C. Sun, H. Huang, M. Feng, X. Shi, X. Zhang and P. Zhou, *Bioorg. Med. Chem. Lett.*, 2006, **16**, 162–166; R. Ronchetti, G. Moroni, A. Carotti, A. Gioiello and E. Camaioni, *RSC Med. Chem.*, 2021, **12**, 1046–1064.

5 H. D. Porter and H. M. Taylor, *US Patent Office*, 3743736, 1973.

6 T. Phuong, T. Khac-Minh, N. T. Van Ha and H. T. Ngoc Phuong, *Bioorg. Med. Chem. Lett.*, 2004, **14**, 653–656.

7 T. J. Egan, K. R. Koch, P. L. Swan, C. Clarkson, D. A. Van Schalkwyk and P. J. Smith, *J. Med. Chem.*, 2004, **47**, 2926–2934.

8 T. Furuta, T. Sakai, T. Senga, T. Osawa, K. Kubo, T. Shimizu, R. Suzuki, T. Yoshino, M. Endo and A. Miwa, *J. Med. Chem.*, 2006, **49**, 2186–2192.

9 A. Solinas, H. Faure, H. Roudaut, E. Traiffort, A. Schoenfelder, A. Mann, F. Manetti, M. Taddei and M. Ruat, *J. Med. Chem.*, 2012, **55**, 1559–1571.

10 M. H. Norman, L. Liu, M. Lee, N. Xi, I. Fellows, N. D. D'Angelo, C. Dominguez, K. Rex, S. F. Bellon, T.-S. Kim and I. Dussault, *J. Med. Chem.*, 2012, **55**, 1858–1867.

11 C. Decroos, C. M. Bowman, J.-A. S. Moser, K. E. Christianson, M. A. Deardorff and D. W. Christianson, *ACS Chem. Biol.*, 2014, **9**, 2157–2164.

12 W.-X. Liu and Y.-B. Jiang, *J. Org. Chem.*, 2008, **73**, 1124–1127.

13 F. A. Saad, N. J. Buurma, A. J. Amoroso, J. C. Knight and B. M. Kariuki, *Dalton Trans.*, 2012, **41**, 4608–4617.

14 H. H. Nguyen, P. C. Thang, A. Rodenstein, R. Kirmse and U. Abram, *Inorg. Chem.*, 2011, **50**, 590–596.

15 M. J. Moloto, M. A. Malik, P. O'Brien, M. Motevalli and G. A. Kolawole, *Polyhedron*, 2003, **22**, 595–603.

16 W. Henderson, B. K. Nicholson, M. B. Dinger and R. L. Bennett, *Inorg. Chim. Acta*, 2002, **338**, 210–218.

17 F. A. Saad, *Spectrochim. Acta, Part A*, 2014, **128**, 386–392.

18 N. Gunasekaran, P. Jerome, S. W. Ng, E. R. T. Tiekink and R. Karvembu, *J. Mol. Catal. A: Chem.*, 2012, **353–354**, 156–162.

19 D. X. West, L. F. Szczepura, J. M. Giesen, W. Kaminsky, J. Kelley and K. I. Goldberg, *J. Mol. Struct.*, 2003, **646**, 95–102.

20 J. Garın, E. Melendez, F. L. Merchan, P. Merino, J. Orduna and T. Tejero, *Synth. Commun.*, 1990, **20**, 2327–2334.

21 B. Vercek, B. Stanovnik and M. Tisler, *Heterocycles*, 1978, **11**, 313–318.

22 D. Saravanabharathi, M. Nethaji and A. G. Samuelson, *Proc. - Indian Acad. Sci., Chem. Sci.*, 2002, **114**, 347–356.

23 A. Saxena, E. C. Dugan, J. Liaw, M. D. Dembo and R. D. Pike, *Polyhedron*, 2009, **28**, 4017–4031.

24 F. Adhami, M. Safavi, M. Ehsani, S. K. Ardestani, F. Emmerling and F. Simyari, *Dalton Trans.*, 2014, **43**, 7945–7957.

25 D. Venkataraman, Y. Du, S. R. Wilson, K. A. Hirsch, P. Zhang and J. S. Moore, *J. Chem. Educ.*, 1997, **74**, 915–918.

26 R. Pattacini, L. Barbieri, A. Stercoli, D. Cauzzi, C. Graiff, M. Lanfranchi, A. Tiripicchio and L. Elviri, *J. Am. Chem. Soc.*, 2006, **128**, 866–876.

27 L. Han, X. Bu, Q. Zhang and P. Feng, *Inorg. Chem.*, 2006, **45**, 5736–5738.

28 C. Lodeiro, J. L. Capelo, E. Bértolo and R. Bastida, *Z. Anorg. Allg. Chem.*, 2004, **630**, 1110–1115.

29 B. J. Hathaway and A. Underhill, *J. Chem. Soc.*, 1961, 3091–3096.
30 I. Ejidike and P. Ajibade, *Molecules*, 2015, **20**, 9788–9802.
31 A. B. P. Lever, *Inorganic Electronic Spectroscopy*, 2nd edn, Elsevier, Amsterdam, 1986, p. 534.
32 World Health Organization, World Malaria Report 2015 http://www.who.int/malaria/publications/world-malaria-report-2015/en/.
33 I. Ullah, R. Sharma, G. A. Biagini and P. Horrocks, *J. Antimicrob. Chemother.*, 2017, **72**, 717–726.
34 D. F. Evans, *J. Chem. Soc.*, 1959, 2003–2005.
35 S. J. Coles and P. A. Gale, *Chem. Sci.*, 2012, **3**, 683.
36 Rigaku, *CrystalClear- SM Expert 3.1 b27*, 2013.
37 Rigaku, *CrysAlisPro, Version 1.171.37.31*, Oxford Diffraction, 2014.
38 G. M. Sheldrick, *Acta Crystallogr., Sect. A: Found. Adv.*, 2015, **71**, 3.
39 O. V. Dolomanov, L. J. Bourhis, R. J. Gildea, J. A. K. Howard and H. Puschmann, *J. Appl. Crystallogr.*, 2009, **42**, 339.
40 W. Kaminsky, K. I. Goldberg and D. X. West, *J. Mol. Struct.*, 2002, **605**, 9–15.